An International Standard Equation of State for the Thermodynamic Properties of HFC-125 (Pentafluoroethane)

Chun-Cheng Piao and Masahiro Noguchi

Mechanical Engineering Laboratory, Daikin Industries, Ltd., 1304 Kanaoka-cho, Sakai, Osaka 591-8511, Japan

Received August 12, 1997; final manuscript received May 7, 1998

An 18-coefficient modified Benedict–Webb–Rubin equation of state for HFC-125 (pentafluoroethane) has been developed. Correlations of vapor pressure and saturated liquid density are also presented. This equation of state has been developed using experimental data for the relationship of pressure-volume-temperature of fluid, saturation properties, isochoric heat capacity data, and speed of sound data. The equation of state is valid in the superheated gaseous phase and the compressed liquid phase at pressures up to 68 MPa, densities to 1700 kg/m^3, and temperatures from the triple point (172.52 K) to 475 K. This equation of state has been selected as an international standard formulation for HFC-125 based on an evaluation of the available equations of state by Annex 18 of the International Energy Agency. © *1998 American Institute of Physics and American Chemical Society.* [S0047-2689(98)00304-3]

Key words: equation of state; heat capacity; HFC-125; pentafluoroethane; thermophysical properties; vapor pressure.

Contents

List of Tables

List of Figures

a)Electronic mail: piao@lab.daikin.co.jp

1. Introduction

HCFC-22 (chlorodifluoromethane) is one of the most widely used working fluids in air conditioning systems. Due to increasing environmental issues, HCFC-22 is scheduled to be phased out before 2030 due to its contribution to ozone depletion. There is no single-component refrigerant to replace HCFC-22 at this moment, although some binary and ternary mixtures have been proposed; e.g., the HFC-32/125 binary and the HFC-32/125/134a ternary systems are considered the most probable substitutes to replace HCFC-22. HFC-125 is included in all of these mixture candidates, and it is important that its properties be known to high accuracy.

We have reported equations of state for HFC-134a [Piao *et al.* (1994)], HCFC-123 [Piao *et al.* (1993)], HFC-32 [Piao and Noguchi (1996a)], and HFC-125 [Piao and Noguchi (1996b)] based on available thermodynamic property measurements. All of these equations of state were developed using the same functional form: an 18-coefficient modified Benedict–Webb–Rubin (BWR) equation of state proposed by Piao *et al.* (1993).

During the last several years, many experimental studies of the thermodynamic properties of HFC-125, i.e., single-phase pressure-volume-temperature (*PVT*) properties, saturation properties, critical parameters, heat capacities, speed of sound, second virial coefficients, and ideal gas heat capacities, have been reported. In this study, an equation of state for HFC-125 is proposed using the most recent information.

It is very important to select standard formulations for use by the refrigeration industry. The recommendation of international standard formulations for the alternative refrigerants has been carried out by Annex 18 (Thermophysical Properties of the Environmentally Acceptable Refrigerants) under the Heat Pump Program of the International Energy Agency (IEA). Phase I of the IEA-Annex 18 resulted in the designation of international standard formulations for HFC-134a [Tillner-Roth and Baehr (1994)] and HCFC-123 [Younglove and McLinden (1994)].

During Phase II, the comparison and evaluation of the available equations of state for HFC-32 and HFC-125 were assigned to an independent group, the IUPAC Thermodynamic Tables Project Center at Imperial College, London, U.K. The IUPAC group presented their final evaluation report (Kilner and Craven, 1996) at the September, 1996 meeting of Annex 18 in Toronto, Canada. The equation of state presented here was chosen as the international standard formulation for HFC-125. The equation of state of Tillner-Roth and Yokozeki (1997) was selected for HFC-32 at the same time.

2. Experimental Data

Eight studies for the critical parameters have been reported as listed in Table 1. All temperature values were converted to ITS-90. A comparison of the different critical parameters is shown in Figs. 1 and 2 on pressure–temperature and temperature–density diagrams.

Kuwabara *et al.* (1995) measured the vapor–liquid coexistence curve and determined the critical temperature and density by observing the disappearing meniscus level and the

TABLE 1. Reported critical parameters for HFC-125

Author	Year	Method[a]	T_c (K)	P_c (kPa)	ρ_c (kg/m^3)	Purity (%)
Singh	1991	1,2,3,4	339.45	3643	571	...
Fukushima	1992	1,3,4	339.18±0.03	3621±3	562±5	99.998
Wilson	1992	2	339.17±0.2	3595±10	571.3±3	99.7
Schmidt	1994	1,2,5	339.33±0.02	...	565±9	99.733
Higashi	1994	1,3,4	339.17±0.01	3620±6	572±6	99.99
Kuwabara	1995	1,3	339.165±0.01	...	568±1	99.99
Piao	1996a	4	(339.165±0.01)[b]	3617.5±3	(568±1)[b]	...
Duarte-Garza	1997b	1,3,4	339.41±0.01	3639.1±0.2	572.3±0.8	99.999

[a]1: Visual observation of the meniscus, 2: rectilinear diameter law, 3: interpolation of the experimental data, 4: extrapolation of the vapor pressure curve, and 5: refractive index.
[b]Values were reported by Kuwabara *et al.* (1995).

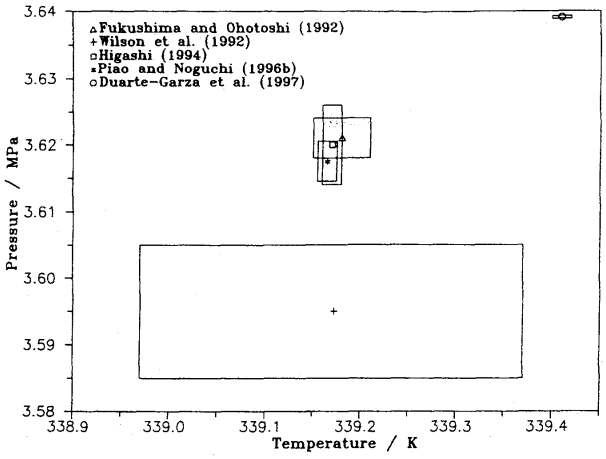

FIG. 1. Comparison of reported critical parameters on a pressure–temperature diagram.

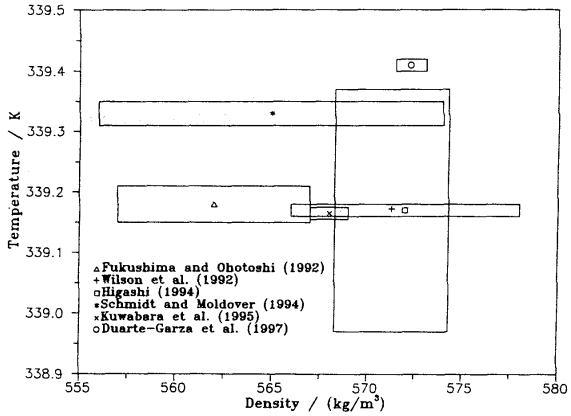

FIG. 2. Comparison of reported critical parameters on a temperature–density diagram.

intensity of the critical opalescence. Singh *et al.* (1991), Fukushima and Ohotoshi (1992), Wilson *et al.* (1992), Schmidt and Moldover (1994), Higashi (1994) and Duarte-Garza and co-workers (1997a,b) also reported critical parameters. The critical temperature reported by Schmidt and Moldover (1994) is about 0.16 K higher than the others and that reported by Duarte-Garza *et al.* (1997b) is about 0.24 K higher than the others. The critical temperature and density proposed by Kuwabara *et al.* (1995) were used in this work,

$$T_c = 339.165 \pm 0.010 \text{ K} \quad (1)$$

and

$$\rho_c = 568 \pm 1 \text{ kg/m}^3. \quad (2)$$

The critical pressure was determined indirectly by extrapolating vapor pressure measurements to the critical temperature,

$$P_c = 3617.5 \pm 3 \text{ kPa}. \quad (3)$$

There are 18 experimental studies available reporting more than 600 vapor pressure measurements for HFC-125. The available vapor pressure measurements are listed in Table 2 and the selected vapor pressure measurements are summarized in Fig. 3. On the basis of the selected vapor pressure measurements in Fig. 3, a vapor pressure correlation for HFC-125 was developed,

TABLE 2. Experimental vapor pressure studies for HFC-125

Author	Year	Temperature (K) Range	Temperature (K) $\pm\delta T$	Purity (%)	No. of Points	Dev. from Eq. (4) (%) Max.	Dev. from Eq. (4) (%) Std.	Dev. from Eq. (7) (%) Max.	Dev. from Eq. (7) (%) Std.
Monluc	1991	303.1–339.1	0.01	99.9	23	−0.175	0.059	−0.195	0.070
Wilson	1992	195.2–339.0	0.005	···	39	1.684	0.537	1.641	0.503
Baroncini	1993	235.7–333.2	0.02	99.8	58	−0.504	0.107	−0.415	0.104
Nagel	1993	205.0–339.4			18	1.025	0.269	0.975	0.279
Sagawa	1994a	313.1–339.1	0.01	99.998	23	−0.265	0.104	−0.272	0.118
Sagawa	1994b	308.1–339.1	0.01	99.998	26	0.065	0.027	0.066	0.025
Weber	1994	175.0–284.7	0.005	99.74	114	−1.014	0.135	−1.107	0.161
Widiatmo	1994	220.0–335.0	0.015	99.8	20	−1.917	0.499	−1.833	0.478
Boyes	1995	273.1–335.2	0.001	99.75	29	0.049	0.017	0.053	0.028
Tsvetkov	1995	263.2–338.1	0.01	99.85	34	0.151	0.053	0.143	0.054
Ye	1995	290.0–339.0	0.01	99.998	12	0.204	0.045	0.148	0.033
Gorenflo	1996	233.2–337.6	···	···	25	0.263	0.064	0.349	0.096
Lueddecke	1996	180.0–250.0	···	99.74	8	−0.100	0.047	−0.187	0.087
Magee	1996	180.0–335.0	0.03	99.74	34	1.319	0.279	1.170	0.247
Oguchi	1996	223.2–338.3	0.005	99.63	61	0.627	0.092	0.690	0.103
de Vries	1997	222.4–339.2	0.005	99.98	98	0.139	0.024	0.199	0.043
Duarte-Garza[a]	1997a	172.5–225.0	···	···	12	−1.336	0.435	−1.378	0.482
Duarte-Garza	1997b	220.0–338.0	0.001	99.999	15	0.766	0.179	0.815	0.198

[a]Derived from internal energy measurements.

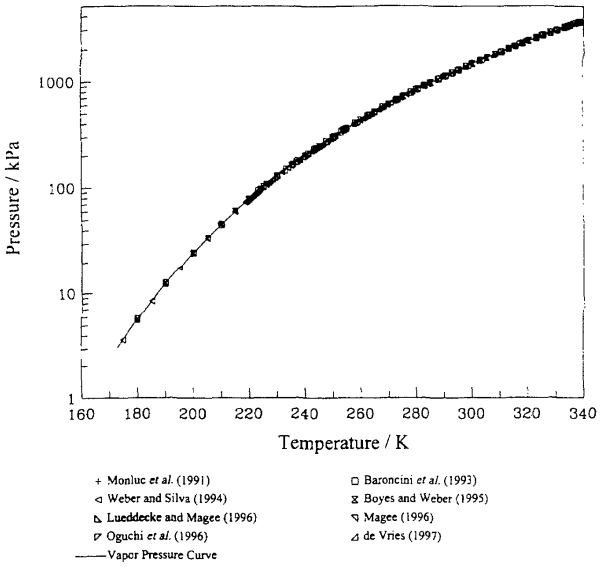

FIG. 3. Summary of selected vapor pressure measurements.

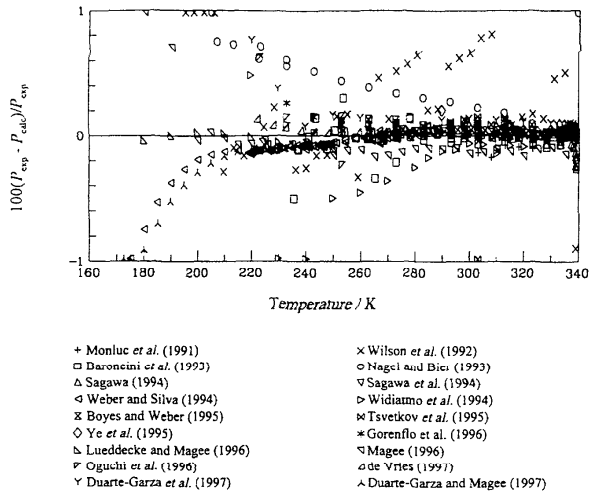

FIG. 4. Comparison of measured vapor pressures and Eq. (4).

$$\ln\left(\frac{P}{P_c}\right)=\frac{T_c}{T}\left[a_1\left(1-\frac{T}{T_c}\right)+a_2\left(1-\frac{T}{T_c}\right)^{1.3}+a_3\left(1-\frac{T}{T_c}\right)^{3}+a_4\left(1-\frac{T}{T_c}\right)^{4}\right]. \quad (4)$$

The coefficients are given in Table 3. The critical temperature and pressure are given in Eqs. (1) and (3). Equation (4) is valid from the triple point [172.52±0.03 K; Lueddecke and Magee (1996)] to the critical temperature, and represents almost all of the selected measurements within ±0.2% as shown in Fig. 4. The maximum and standard deviations of the reported measurements from Eq. (4) are also given in Table 2. The percent deviation is defined as $\%\Delta P = 100[(P_{\rm exp}-P_{\rm cal})/P_{\rm exp}]$, and the standard deviation is defined as $\%\sigma P = 100[\Sigma\{(P_{\rm exp}-P_{\rm cal})/P_{\rm exp}\}^2/(n-1)]^{1/2}$.

Five studies for the saturated liquid and vapor densities of HFC-125 reported 87 values. The available saturated liquid densities measurements are summarized in Table 4 and Fig. 5. Based on these measurements, a correlation of the saturated liquid density has been developed,

$$\frac{\rho}{\rho_c}=1+b_1\left(1-\frac{T}{T_c}\right)^{0.325}+b_2\left(1-\frac{T}{T_c}\right)^{0.6}+b_3\left(1-\frac{T}{T_c}\right)+b_4\left(1-\frac{T}{T_c}\right)^{3}. \quad (5)$$

TABLE 3. Coefficients of Eqs. (4) and (5)

i	a_i	b_i
1	−7.671 281 367 03	1.777 409 634 98
2	1.292 524 476 51	0.566 934 114 78
3	−2.103 362 807 47	0.333 737 378 064
4	−1.905 498 791 01	0.262 031 546 374

The critical temperature and density are given in Eqs. (1) and (2). The coefficients of Eq. (5) are listed in Table 3. This correlation is applicable for temperatures from the triple point to the critical point. Equation (5) represents almost all of the available saturated liquid densities within ±0.2%, except those in the vicinity of the critical point as shown in Fig. 6 and Table 4.

More than 2000 experimental *PVT* data points have been reported by 12 papers since 1991, as summarized in Table 5 and Fig. 7. The available experimental data cover a wide range of temperatures from 178 to 473 K, densities up to 1700 kg/m^3, and pressures up to 68 MPa.

Lueddecke and Magee (1996) reported 99 isochoric heat capacity points for the liquid phase and 93 heat capacity points for the saturated liquid. Wilson *et al.* (1992) and Kan *et al.* (1996) reported 10 and 78 isobaric heat capacity data points, respectively, mostly in the compressed liquid phase. Hozumi *et al.* (1996) and Gillis (1997) reported 72 and 149 speed of sound data points in the vapor phase, and Grebenkov *et al.* (1994) and Takagi (1996) reported 30 and 167 speed of sound data points in the liquid phase, respectively. Kraft and Leipertz (1994) reported 21 speed of sound data points along the saturated liquid and vapor boundaries. The heat capacity and speed of sound measurements are summarized in Table 6 and Fig. 8. Published values for the second virial coefficients are summarized in Table 7.

3. Ideal Gas Heat Capacity

The correlation of the ideal gas heat capacity reported by Hozumi *et al.* (1996) was adopted in this study,

$$C_p^0/R_0=d_1+d_2T+d_3T^2, \quad (6)$$

where $R_0=8.314471$ kJ/(kmol K) and the coefficients are given in Table 8. Published values of the ideal gas heat ca-

TABLE 4. Experimental studies of saturated liquid and vapor densities for HFC-125

Author	Year	Temperature (K) Range	Temperature (K) $\pm \delta T$	Purity (%)	No. of Points	Dev. From Eq. (5) (%) Max.	Dev. From Eq. (5) (%) Std.	Dev. From Eq. (7) (%) Max.	Dev. From Eq. (7) (%) Std.
Defibaugh	1992	275.6–337.8	0.01	99.9	9	2.907	1.003	1.705	0.590
Higashi	1994	324.6–339.2	0.01	99.99	9	0.504	0.294	−3.396	1.390
Widiatmo	1994	220.0–335.0	0.015	99.8	25	−0.427	0.122	−0.256	0.057
Kuwabara	1995	331.5–339.2	0.01	99.8	16	−5.089	1.441	−7.799	2.682
Magee	1996	173.5–308.5	0.03	99.74	7	0.122	0.024	0.152	0.074
Higashi	1994	326.9–339.2	0.01	99.99	8	...	...	13.302	4.661
Kuwabara	1995	335.8–339.2	0.01	99.8	13	...	...	10.386	4.845

pacity are summarized in Table 9. Figure 9 shows comparisons of the ideal gas heat capacity values with values calculated from Eq. (6).

4. Modified BWR Equation of State

We have published an 18-coefficient mBWR equation of state for HCFC-123 [Piao *et al.* (1993)]. This equation of state has 18 coefficients and is valid over a wide temperature and pressure range. The format of this equation of state was also applied to HFC-134a [Piao *et al.* (1994)], HFC-32 [Piao and Noguchi (1996a)], and HFC-125 [Piao and Noguchi (1996b)] with very good results.

In this study, we revised our equation of state [Piao and Noguchi (1996b)] by using new and updated measurements. Vapor pressure calculations were also improved according to a recommendation of the IEA Annex 18.

The equation of state was developed based on the available measurements by a least square fitting method. The input data of the least square fitting procedure included *PVT* data, saturation data (Maxwell's equal area principle), critical point constraints, isochoric heat capacities, and speed of sound data. The critical point constraints include the conditions that the calculated pressure at the critical temperature and density is equal to the critical pressure, and that the first and second differentials of pressure with respect to density at constant temperature are zero at the critical point. The saturation data, i.e., vapor pressures coupled with saturated vapor and liquid densities, and the Maxwell's equal area principle, i.e., the thermodynamic restriction that the Gibbs free energy of the saturated liquid and vapor values are equal at the same temperatures, were calculated from Eqs. (4) and (5), and a supplementary correlation for the saturated vapor density developed in the present study. This was done since it is difficult to obtain vapor pressure data and saturated liquid and vapor densities at exactly the same temperature. The saturated vapor density correlation was developed based mainly on data calculated from Eq. (4) and a simple but highly accurate supplementary equation of state for the superheated gaseous phase and supercritical region. The isochoric heat capacity measurements were used directly in the fitting procedure. The isobaric heat capacity data and speed of sound data were used indirectly in the fitting procedure. The equation of state was fitted without the isobaric heat capacity data and speed of sound data initially. Data for the first derivative of pressure with respect to density were then derived from speed of sound data using the equation of state and were included in the fitting procedure. These data were updated when the behavior of isochoric and isobaric heat capacities improved.

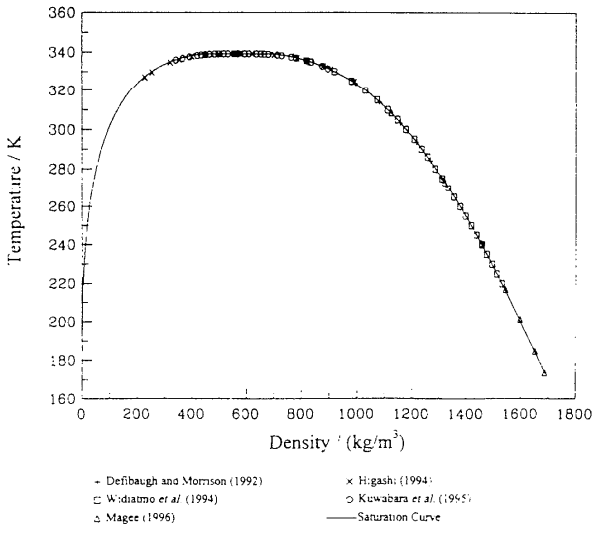

FIG. 5. Summary of reported saturated liquid and vapor densities.

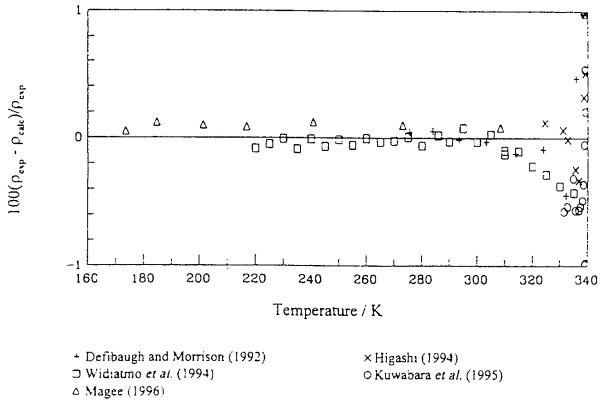

FIG. 6. Comparison of measured saturated liquid densities and Eq. (5).

TABLE 5. Summary of reported *PVT* measurements for HFC-125

Author	Year	Method[a]	P (MPa) Range	P (MPa) $\pm\delta P$	ρ (kg/m^3) Range	ρ (kg/m^3) $\pm\delta\rho$	T (K) Range	T (K) $\pm\delta T$	Purity (%)	No. of Points
Monluc	1991	2	1.6–11.1	0.002	97–940	0.1%	310–423	0.01	99.9	50
Defibaugh	1992	3	1.6–6.3	0.0005	258–1348	0.05%	275–369	0.01	99.9	162
Wilson	1992	2	1.7–10.4	0.25%	107–1627	···	198–448	0.05	99.7	84
Baroncini	1993	2	1.0–2.5	0.0005	60–155	0.2	293–338	0.01	99.8	58
Sagawa	1994a	2	0.7–11.8	0.002	36–1065	0.1%	308–423	0.001	99.9	211
Boyes	1995	1	0.3–4.6	0.0001	14–340	···	273–363	0.001	99.75	92
Tsvetkov	1995	2	0.6–6.1	0.02%	37–517	···	273–443	0.01	99.85	44
Magee	1996	2	3.6–35.4	0.05%	1115–1684	0.05%	178–398	0.03	99.74	77
Oguchi	1996	2	0.8–17.0	0.0025	51–1145	0.01%	280–473	0.005	99.63	167
Zhang	1996	1	0.1–3.6	0.008	5–229	0.15%	290–390	0.008	99.9	93
de Vries	1997	1,3	0.02–19.8	0.0001	1–1510	0.03%	243–413	0.005	99.97	962
Duarte-Garza	1997b	1,2	1.2–67.9	0.01	914–1699	0.1%	180–350	0.01	99.999, 99.2	148

[a]1: Burnett method, 2: isochoric method, and 3: vibrating tube method.

The nondimensional form of the 18-coefficient mBWR equation of state developed in this work for R-125 is

$$P_r = T_r\rho_r/Z_c + B_1\rho_r^2 + B_2\rho_r^3 + B_3\rho_r^4 + B_4\rho_r^5 + B_5\rho_r^6 + B_6\rho_r^7 + (B_7 + B_8\rho_r^2)\rho_r^3 \exp(-\rho_r^2), \quad (7)$$

where

$$B_1 = c_1T_r + c_2 + c_3/T_r^2 + c_4/T_r^3,$$

$$B_2 = c_5T_r + c_6 + c_7/T_r^2,$$

$$B_3 = c_8 + c_9/T_r^2,$$

$$B_4 = c_{10} + c_{11}/T_r,$$

$$B_5 = c_{12} + c_{13}/T_r,$$

$$B_6 = c_{14},$$

$$B_7 = c_{15} + c_{16}/T_r,$$

$$B_8 = c_{17} + c_{18}/T_r,$$

and where $P_r = P/P_c$, $\rho_r = \rho/\rho_c$, $T_r = T/T_c$, $Z_c = P_c/(RT_c\rho_c)$, $R = R_0/M$, $R_0 = 8.314471$ kJ/(kmol K), and $M = 120.022$ kg/kmol. The coefficients of the equation of state are listed in Table 10.

It should be noted that the calculated critical parameters from the equation of state, Eq. (7), are slightly different from the critical parameters adopted in this study. As mentioned above, the critical parameters and the first and second differentials of pressure with respect to density were treated as inputs similar to other data, e.g., *PVT* data, vapor pressure data, etc., but have much higher weighting factors compared to the other data points. Consequently, it was difficult to force the equation of state to go through the critical point exactly, and reproduce other properties as well.

5. Discussion

5.1. Saturation Boundary

Figure 10 shows comparisons of measured vapor pressures with the equation of state. The vapor pressure correlation, Eq. (4), is shown as the solid curve. The equation of state represents most of the measurements within $\pm 0.1\%$, except at temperatures below 200 K. The vapor pressure ancillary equation, Eq. (4), was represented within $\pm 0.1\%$, from the triple point to the critical point. Details of the comparisons are summarized in Table 2.

Figures 11 and 12 show comparisons of saturated liquid and vapor densities with the equation of state. The saturated liquid correlation, Eq. (5), is shown as the solid curve. The reported saturated liquid densities are represented by the equation of state within $\pm 0.2\%$, except for several data in the vicinity of the critical region. The saturated vapor densities show large deviations from the equation of state. The results of the comparisons are also summarized in Table 4.

5.2. Single-Phase *PVT* Data and Second Virial Coefficients

Figure 13 shows comparisons of measured *PVT* data and the equation of state for the superheated gaseous phase and the supercritical region. The numerical results of the comparisons are summarized in Table 11. For the compressed liquid phase, the comparisons are shown in Fig. 14 as density deviations, and the results are given in Table 11.

Figures 15 and 16 compare the second virial coefficients calculated from the equation of state with reported data by Bignell and Dunlop (1993), Boyes and Weber (1995), Ye *et al.* (1995), Zhang *et al.* (1995), Hozumi *et al.* (1996), and Gillis (1997). The equation of state agrees well with the results of Hozumi *et al.* (1996). Other measurements are represented within $\pm 3.8\%$.

TABLE 6. Summary of reported heat capacity and speed of sound data for HFC-125

Author	Year	Phase	P (MPa) Range	$\pm \delta P$	T (K) Range	$\pm \delta T$	Heat capacity (kJ/kg K) Range	$\pm \delta C$	Purity (%)	Points
Lueddecke, C_v	1996	Liquid	3.8–33	···	200–342	···	0.71–0.87	0.7%	99.74	99
Lueddecke, C_{sat}	1996	Liquid	0.004–0.8	···	176–278	···	1.04–1.26	0.7%	99.74	93
Kan, C_p	1996	Liquid	1.6–3.0	0.1%	276–328	0.02	1.25–2.15	0.2%	99.9	78
Wilson, C_p	1992	V/L	0.1–3.5	0.005	216–333	0.02	0.69–1.71	5%	99.66	10
							Speed of sound w (m/s) Range	$\pm \delta w$		
Kraft	1994	Vapor	1.7–3.5	···	307–388	0.05	81–112	0.5%	99.99	9
Hozumi	1996	Vapor	0.01–0.25	0.0005	273–343	0.011	142–161	0.01%	99.998	72
Gillis	1997	Vapor	0.04–1.0	0.000 08	240–400	0.1	130–171	0.01%	99.85	149
Grebenkov	1994	Liquid	1.1–16	0.1%	288–333	0.02	301–540	0.2%	99.9	30
Kraft	1994	Liquid	1.2–3.6	···	293–338	0.05	85–354	0.5%	99.99	13
Takagi	1996	Liquid	0.2–32	0.005	241–333	0.02	278–777	5%	99.66	167

5.3. Heat Capacity and Speed of Sound Data

The equation of state represents the C_p data reported in the liquid phase by Wilson *et al.* (1992) and Kan *et al.* (1996) with maximum deviations of −3.41% and 2.65%, and standard deviations of 1.60% and 0.44%, respectively, as shown in Fig. 17. The C_v data reported in liquid phase by Lueddecke and Magee (1996) are also represented with a maximum deviation of −1.54% and a standard deviation of 0.57%, as shown in Fig. 18. The C_{sat} data reported for the saturated liquid by Lueddecke and Magee (1996) are represented with a maximum deviation of −1.76% and a standard deviation of 0.75%. Figures 19 and 20 show comparisons of speed of sound data with the equation of state. The speed of sound data reported in the superheated gaseous phase by Hozumi *et al.* (1996) are represented with a maximum deviation of 0.044% and a standard deviation of 0.012%. The speed of sound data in the superheated gaseous phase reported by Gillis (1997) are represented with a maximum deviation of 0.23% and a standard deviation of 0.056%. The speed of sound in the liquid phase by Takagi (1996) and by Grebenkov *et al.* (1994) are represented with maximum deviations of 1.50% and 0.54%, and standard deviations of 0.50% and 0.21%, respectively. The speed of sound at saturation by Kraft and Leipertz (1994) are represented with a maximum deviation of −9.38% and a standard deviation of 3.35%.

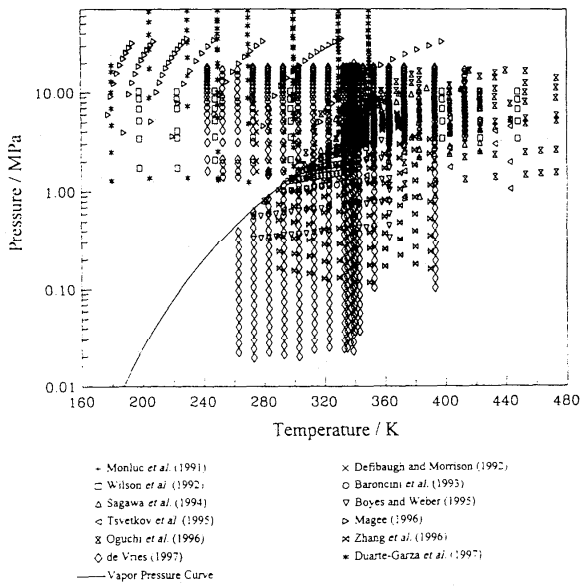

FIG. 7. Summary of reported PVT measurements.

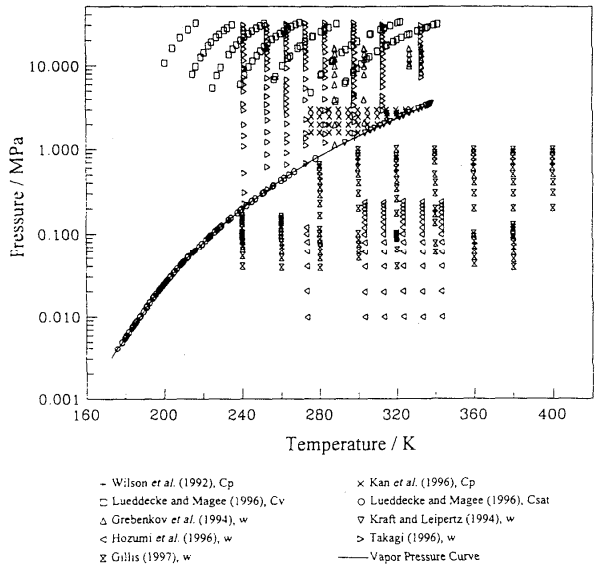

FIG. 8. Summary of reported heat capacity and speed of sound measurements.

TABLE 7. Summary of second virial coefficients for HFC-125

Author	Year	T (K) Range	$-B$ (dm^3/kg) Range	$\pm \delta B$	Purity	No. of Points
Bignell	1993	290–310	2.8–3.3	···	98.0	3
Boyes	1995	280–350	2.1–3.6	···	99.75	8
Ye	1995	290–390	1.6–3.4	···	99.998	11
Zhang	1995	290–390	1.5–3.3	4%	99.9	11
Gillis	1997	240–400	1.4–5.3	0.6%	99.95	9

5.4. Pressure–Temperature Behavior of Heat Capacity and Speed of Sound

The mBWR equation of state presented here represents the experimental data over the entire fluid phase. Figures 21, 22 and 23 show the behavior of the isobaric heat capacity, isochoric heat capacity, and speed of sound calculated from the equation of state. We can examine the quality of the thermodynamic surface derived from the mBWR from the behavior of these properties. The isobars shown in Fig. 21 show very smooth behavior both in the gaseous and liquid phases. For the isochoric heat capacity, isobars cross around 240 K in the liquid phase. The speed of sound does not go to zero at the critical point, a common defect of analytical equations of state. The behavior of the heat capacities and the speed of sound are not represented accurately in the immediate vicinity of the critical point. Other than these few exceptions, the thermodynamic property surface is represented very well.

6. Summary and Conclusions

An 18-coefficient mBWR equation of state for HFC-125 has been developed. New correlations for the vapor pressure and saturated liquid density are also presented. This equation of state is valid from the triple point to 475 K, at densities up to 1700 kg/m^3 state and pressures up to 68 MPa over the entire fluid phase.

This equation of state has been selected as the international standard formulation for HFC-125, based on an evaluation of the available equations of state by IEA-Annex 18.

7. Acknowledgments

The authors thank Professor Koichi Watanabe at Keio University, Yokohama, Japan for his valuable advice. The authors also thank Dr. Eric Lemmon at the National Institute of Standards and Technology, Boulder, Colorado for his devoted assistance and appropriate advice during the development of the equation of state and preparing the manuscript.

TABLE 8. Coefficients for the ideal gas heat capacity

i	d_i
1	4.3987
2	0.0242728
3	-4.099×10^{-6}

8. Appendix A: Derived Properties

The pressure is calculated from the Helmholtz free energy a using

$$P=-\left(\frac{\partial a}{\partial v}\right)_T, \tag{A1}$$

from which the Helmholtz energy is calculated using

$$a=-\int_\infty^v\left(P-\frac{RT}{v}\right)dv-RT\ln(v)+a_v^0$$

$$=-\int_0^\rho\frac{P-R\rho T}{\rho^2}d\rho+RT\ln(\rho)+a_v^0, \tag{A2}$$

where the superscript 0 denotes the ideal gas state. The entropy s, internal energy u, enthalpy h, and Gibbs free energy g are given as

$$s=-\left(\frac{\partial a}{\partial T}\right)_v=-\left(\frac{\partial a}{\partial T}\right)_\rho, \tag{A3}$$

$$u=a+Ts=a-T\left(\frac{\partial a}{\partial T}\right)_\rho, \tag{A4}$$

$$h=u+Pv=a-T\left(\frac{\partial a}{\partial T}\right)_\rho+\frac{P}{\rho}, \tag{A5}$$

and

$$g=a+Pv=a+\frac{P}{\rho}. \tag{A6}$$

The isochoric heat capacity C_v, the isobaric heat capacity C_p, and the speed of sound w are given by

TABLE 9. Summary of ideal gas heat capacity data for HFC-125

Author	Year	Method[a]	T (K) Range	C_p^0 (kJ/kg K) Range	(%)	Purity (%)	No. of Points
Chen	1975	1	100–1500	0.42–1.4		···	18
Hozumi	1996	2	273–343	0.74–0.85	0.1%	99.998	6
Gillis	1997	2	240–380	0.69–0.91	0.1%	99.95	8

[a]1: Rigid-rotor harmonic-oscillator approximation, and 2: derived from speed of sound data.

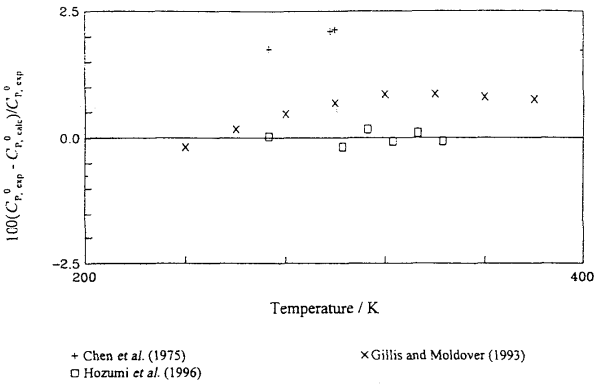

FIG. 9. Comparison of ideal gas heat capacity values and Eq. (6).

$$C_v=\left(\frac{\partial u}{\partial T}\right)_v=T\left(\frac{\partial s}{\partial T}\right)_\rho=-T\left(\frac{\partial^2 a}{\partial T^2}\right)_\rho, \tag{A7}$$

$$C_P=\left(\frac{\partial h}{\partial T}\right)_P=C_v+\frac{T}{\rho^2}\left(\frac{\partial P}{\partial T}\right)_\rho^2\Big/\left(\frac{\partial P}{\partial \rho}\right)_T, \tag{A8}$$

$$w=\left[-v^2\left(\frac{\partial P}{\partial v}\right)_T\frac{C_P}{C_v}\right]^{1/2}=\left[\left(\frac{\partial P}{\partial \rho}\right)_T\frac{C_P}{C_v}\right]^{1/2}. \tag{A9}$$

Finally, the Joule–Thomson coefficient μ, and the isentropic expansion exponent κ are given by

$$\mu=\left(\frac{\partial T}{\partial P}\right)_h=\frac{1}{C_P}\left[T\left(\frac{\partial v}{\partial T}\right)_P-v\right]$$

$$=\frac{1}{C_P\rho}\left[\frac{T}{\rho}\left(\frac{\partial P}{\partial T}\right)_\rho\Big/\left(\frac{\partial P}{\partial \rho}\right)_T-1\right], \tag{A10}$$

$$\kappa\approx-\frac{v}{P}\left(\frac{\partial P}{\partial v}\right)_T\frac{C_P}{C_v}=w^2\frac{\rho}{P}. \tag{A11}$$

TABLE 10. Coefficients of the equation of state

i	m_i	n_i	c_i
1	2	−1	0.951 124 690 482
2	2	0	−2.711 581 535 49
3	2	2	−2.905 027 115 98
4	2	3	−0.070 211 796 610 4
5	3	−1	2.865 199 781 28
6	3	0	−4.662 342 325 81
7	3	2	4.602 879 948 33
8	4	0	1.216 585 133 3
9	4	2	−1.099 103 680 83
10	5	0	−0.154 355 762 519
11	5	1	−1.136 251 778 13
12	6	0	0.276 370 825 11
13	6	1	0.307 380 467 447
14	7	0	−0.040 172 984 196 3
15	0	0	3.662 403 539 29
16	0	1	−4.325 506 941 04
17	2	0	−3.032 348 051 31
18	2	1	3.342 274 905 86

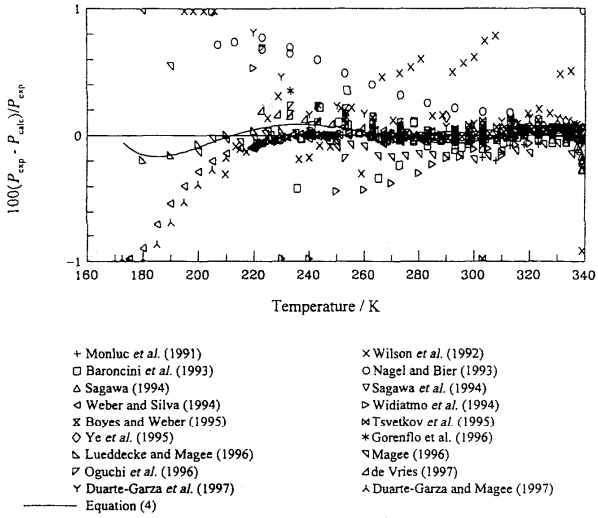

FIG. 10. Comparison of measured vapor pressures and Eq. (7).

The Helmholtz free energy in the ideal gas state is calculated using

$$a_v^0=u^0-Ts^0, \tag{A12}$$

$$u^0=\int_{T_0}^{T}C_v^0dT+C_u=\int_{T_0}^{T}(C_P^0-R)dT+C_u, \tag{A13}$$

$$s^0=\int_{T_0}^{T}\frac{C_v^0}{T}dT+C_s=\int_{T_0}^{T}\frac{(C_P^0-R)}{T}dT+C_s. \tag{A14}$$

T_0 is a reference temperature, and C_u and C_s are constants of the integration from the reference temperature. The International Institute of Refrigeration standard was adopted here by setting the enthalpy and the entropy to 200 kJ/kg and 1 kJ/(kg K), respectively, at 0 °C for the saturated liquid. The corresponding values for the constants of integration are C_u = 324.932 13 kJ/kg and C_s = 1.324 298 3 kJ/(kg K).

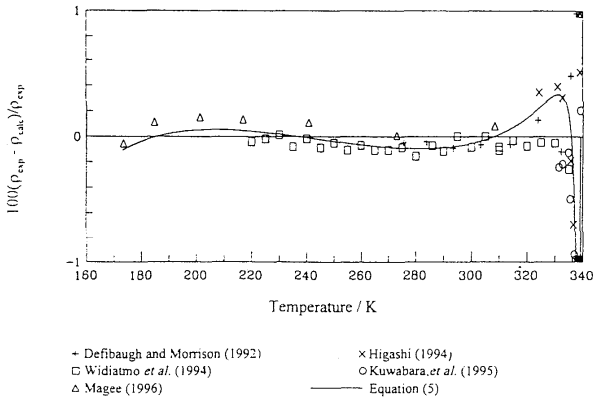

FIG. 11. Comparison of measured saturated liquid densities and Eq. (7).

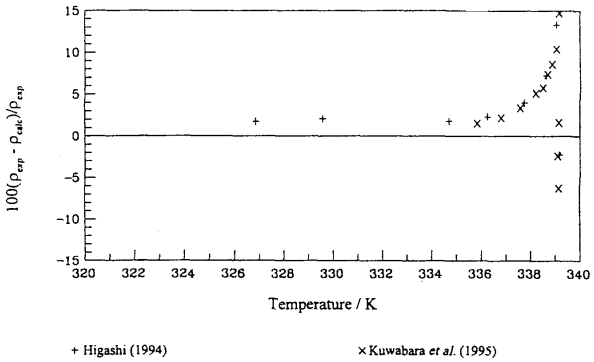

FIG. 12. Comparison of measured saturated vapor densities and Eq. (7).

All of the thermodynamic quantities used in engineering calculations can be calculated from these fundamental functions, Eqs. (A1)–(A14).

The core functions used in Eqs. (A1)–(A14) are given as follows. The partial derivative of pressure with respect to temperature is given by

$$\left(\frac{\partial P}{\partial \rho}\right)_T = \frac{P_c}{\rho_c}\left(\frac{\partial P_r}{\partial \rho_r}\right)_{T_r}, \tag{A15}$$

$$\left(\frac{\partial P_r}{\partial \rho_r}\right)_{T_r} = \frac{T_r}{Z_c} + \sum_{i=1}^{14} c_i m_i \frac{\rho_r^{m_i-1}}{T_r^{n_i}} + \sum_{i=15}^{18} c_i (m_i + 3 - 2\rho_r^2) \frac{\rho_r^{m_i+2}}{T_r^{n_i}} \exp(-\rho_r^2). \tag{A16}$$

The partial derivative of pressure with respect to density is given by

$$\left(\frac{\partial P}{\partial T}\right)_\rho = \frac{P_c}{T_c}\left(\frac{\partial P_r}{\partial T_r}\right)_{\rho_r}, \tag{A17}$$

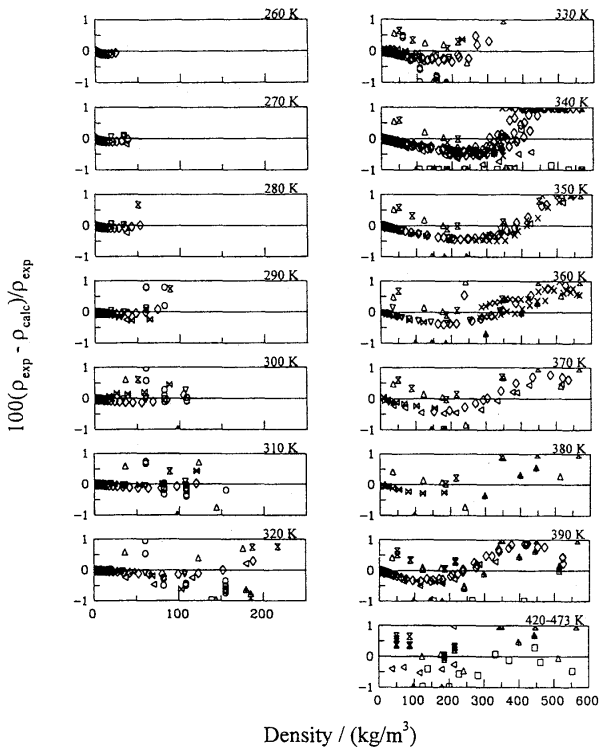

FIG. 13. Comparison of *PVT* measurements and Eq. (7) in the gaseous phase and supercritical region.

$$\left(\frac{\partial P_r}{\partial T_r}\right)_{\rho_r} = \frac{\rho_r}{Z_c} - \sum_{i=1}^{14} c_i n_i \frac{\rho_r^{m_i}}{T_r^{n_i+1}} - \sum_{i=15}^{18} c_i n_i \frac{\rho_r^{m_i+3}}{T_r^{n_i+1}} \exp(-\rho_r^2). \tag{A18}$$

TABLE 11. Summary of comparisons of reported *PVT* measurements and the equation of state

Author	Year	$d\rho/\rho$ (%) (ρ<600 kg/m^3) Max.	Dev.	No. of Points Stand. Dev	Bad data (>10%)	$d\rho/\rho$ (%) (500 kg/m^3<ρ<1700 kg/m^3) Max.	Dev.	No. of Points Stand. Dev	Bad data (>10%)
Monluc	1991	3.186	1.268	31	0	−1.370	0.390	19	0
Defibaugh	1992	5.887	1.177	74	2	5.887	0.945	105	2
Wilson	1992	−3.146	0.801	29	2	−2.197	0.535	59	3
Baroncini	1993	−1.137	0.508	58	0	···	···	0	0
Sagawa	1994[b]	−7.600	1.467	134	5	−7.600	1.215	119	5
Boyes	1995	−0.389	0.137	92	0	···	···	0	0
Tsvetkov	1995	2.325	0.601	44	1	1.748	0.671	3	0
Magee	1996	···	···	0		−0.104	0.057	77	0
Oguchi	1996	4.957	0.997	98	0	−6.535	1.380	85	2
Zhang	1996	−0.623	0.162	93	0	···	···	0	0
de Vries	1997	8.942	0.856	491	0	8.304	0.772	495	0
Duarte-Garza	1997[b]	···	···	0		−0.336	0.087	148	0

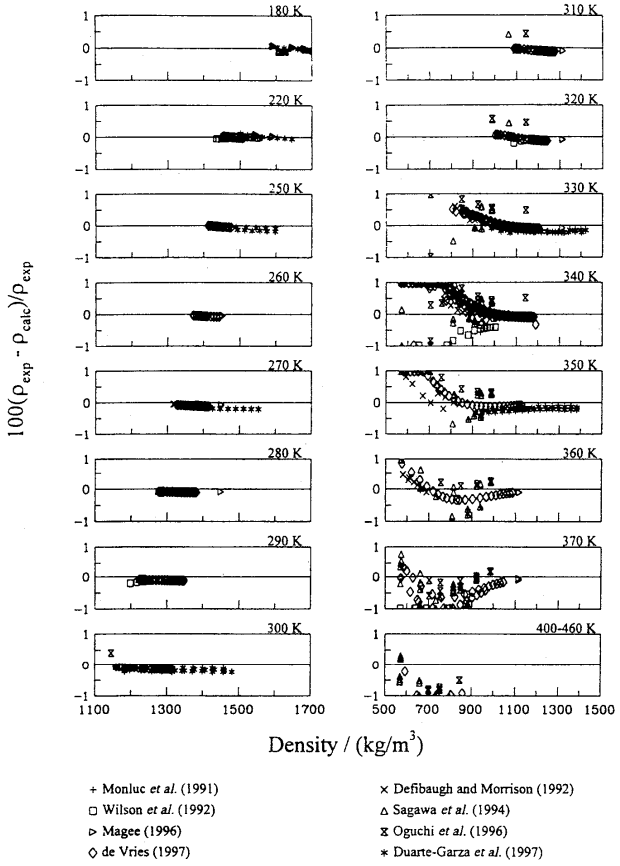

FIG. 14. Comparison of *PVT* measurements and Eq. (7) in the liquid phase and supercritical region.

The Helmholtz free energy calculated from the mBWR equation of state is

$$a = a^R + a_v^0 = T_c R Z_c a_r^R + a_v^0, \tag{A19}$$

$$a_r^R = \sum_{i=1}^{14} c_i \frac{1}{m_i - 1} \frac{\rho_r^{m_i - 1}}{T_r^{n_i}} + \sum_{i=15}^{16} \frac{1}{2} \frac{c_i}{T_r^{n_i}} [1 - \exp(-\rho_r^2)] + \sum_{i=17}^{18} \frac{1}{2} \frac{c_i}{T_r^{n_i}} [1 - (1 + \rho_r^2)\exp(-\rho_r^2)] + \frac{T_r}{Z_c} \ln(\rho_r), \tag{A20}$$

$$a_v^0 = u^0 - T s^0 \tag{A21}$$

$$u^0 = \int_{T_0}^{T} (C_P^0 - R) dT + C_u = R\left[(d_1 - 1)(T - T_0) + \frac{d_2}{2}(T^2 - T_0^2) + \frac{d_3}{3}(T^3 - T_0^3) \right] + C_u. \tag{A22}$$

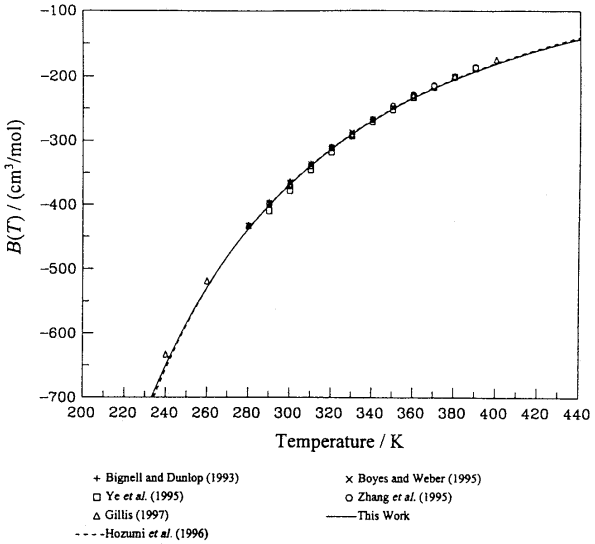

FIG. 15. Temperature dependence of the second virial coefficient.

$$s^0 = \int_{T_0}^{T} \frac{C_v^0}{T} dT + C_s = \int_{T_0}^{T} \frac{(C_P^0 - R)}{T} dT + C_s = R\left[(d_1 - 1)\ln\frac{T}{T_0} + d_2(T - T_0) + \frac{d_3}{2}(T^2 - T_0^2) \right] + C_s. \tag{A23}$$

The first partial derivative of Helmholtz free energy with respect to temperature is given by

$$\left(\frac{\partial a}{\partial T}\right)_\rho = \left(\frac{\partial a^R}{\partial T}\right)_\rho + \left(\frac{da_v^0}{dT}\right), \tag{A24}$$

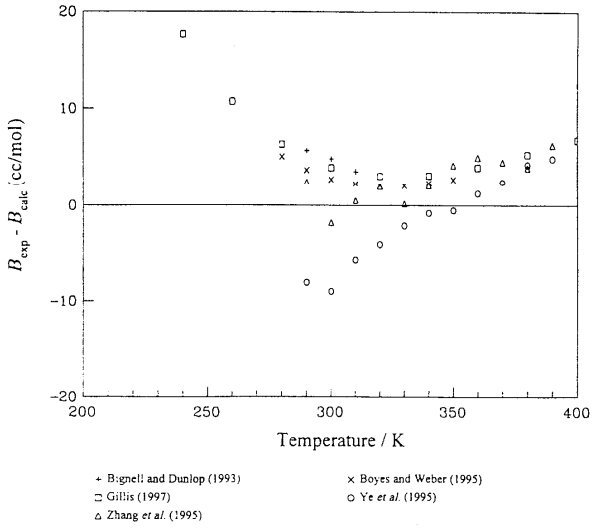

FIG. 16. Comparison of second virial coefficient measurements and Eq. (7).

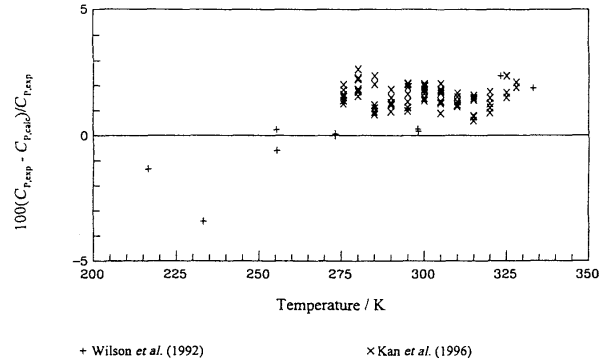

FIG. 17. Comparison of measured C_p data and Eq. (7).

$$\left(\frac{\partial a^R}{\partial T}\right)_\rho = T_c R Z_c \left(\frac{\partial a_r^R}{\partial T_r}\right)_{\rho_r}, \tag{A25}$$

$$\left(\frac{da_v^0}{dT}\right) = \left(\frac{du^0}{dT}\right) - T\left(\frac{ds^0}{dT}\right) - s^0, \tag{A26}$$

where

$$\left(\frac{\partial a_r^R}{\partial T_r}\right)_{\rho_r} = \sum_{i=1}^{14} c_i \frac{-n_i}{m_i - 1} \frac{\rho_r^{m_i-1}}{T_r^{n_i+1}} - \sum_{i=15}^{16} c_i \frac{n_i}{2} \frac{1}{T_r^{n_i+1}} \times [1 - \exp(-\rho_r^2)] - \sum_{i=17}^{18} c_i \frac{n_i}{2} \frac{1}{T_r^{n_i+1}} \times [1 - (1+\rho_r^2)\exp(-\rho_r^2)] + \frac{1}{Z_c} \ln(\rho_r), \tag{A27}$$

$$\frac{du^0}{dT} = R[(d_1 - 1) + d_2 T + d_3 T^2], \tag{A28}$$

$$\frac{ds^0}{dT} = R\left[\frac{d_1 - 1}{T} + d_2 + d_3 T\right]. \tag{A29}$$

The second partial derivative of Helmholtz free energy with respect to temperature is given by

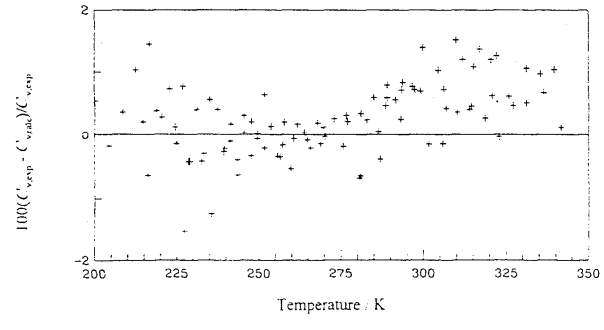

FIG. 18. Comparison of measured C_v data and Eq. (7).

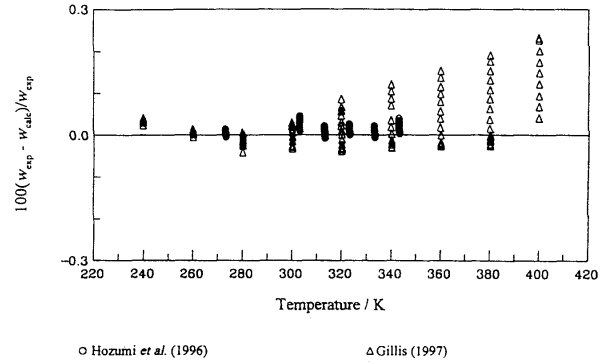

FIG. 19. Comparison of measured speed of sound data and Eq. (7) in the vapor phase.

$$\left(\frac{\partial^2 a}{\partial T^2}\right)_\rho = \left(\frac{\partial^2 a^R}{\partial T^2}\right)_\rho + \left(\frac{d^2 a_v^0}{dT^2}\right), \tag{A30}$$

$$\left(\frac{\partial^2 a^R}{\partial T^2}\right)_\rho = T_c R Z_c \left(\frac{\partial^2 a_r^R}{\partial T_r^2}\right)_{\rho_r}, \tag{A31}$$

$$\left(\frac{d^2 a_v^0}{dT^2}\right) = \left(\frac{d^2 u^0}{dT^2}\right) - 2\left(\frac{ds^0}{dT}\right) - T\left(\frac{d^2 s^0}{dT^2}\right), \tag{A32}$$

where

$$\left(\frac{\partial^2 a_r^R}{\partial T_r^2}\right)_{\rho_r} = \sum_{i=1}^{14} c_i \frac{n_i(n_i+1)}{m_i - 1} \frac{\rho_r^{m_i-1}}{T_r^{n_i+2}} - \sum_{i=15}^{16} c_i \frac{n_i(n_i+1)}{2} \frac{1}{T_r^{n_i+2}} [1 - \exp(-\rho_r^2)] - \sum_{i=17}^{18} c_i \frac{n_i(n_i+1)}{2} \frac{1}{T_r^{n_i+2}} \times [1 - (1+\rho_r^2)\exp(-\rho_r^2)], \tag{A33}$$

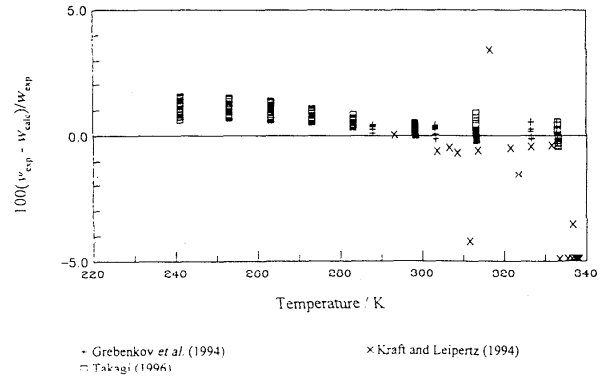

FIG. 20. Comparison of measured speed of sound data and Eq. (7) in the liquid phase and along the saturation boundaries.

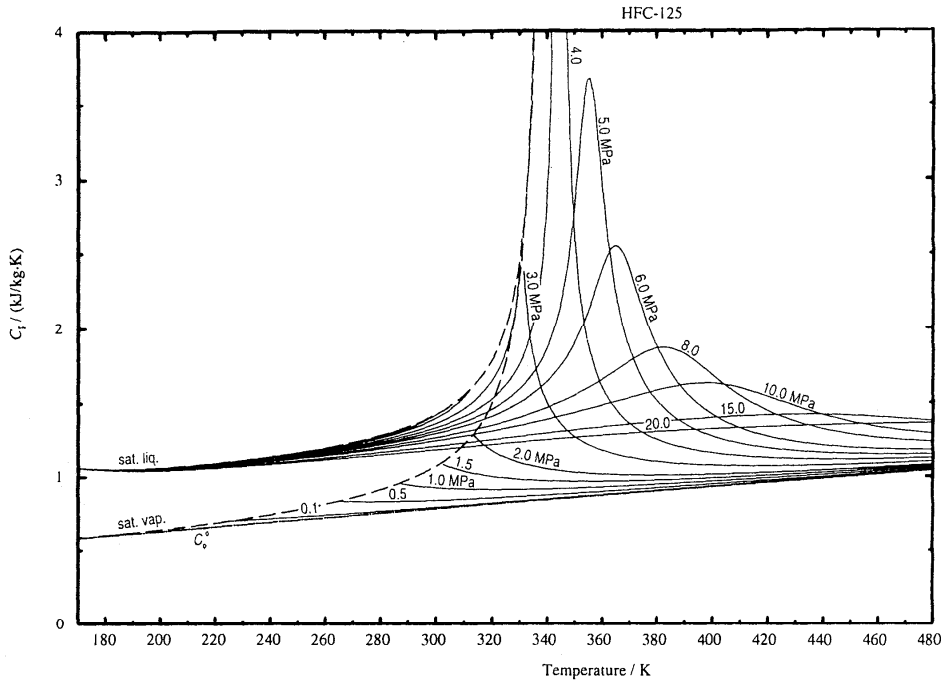

FIG. 21. Temperature dependence of isobaric heat capacity.

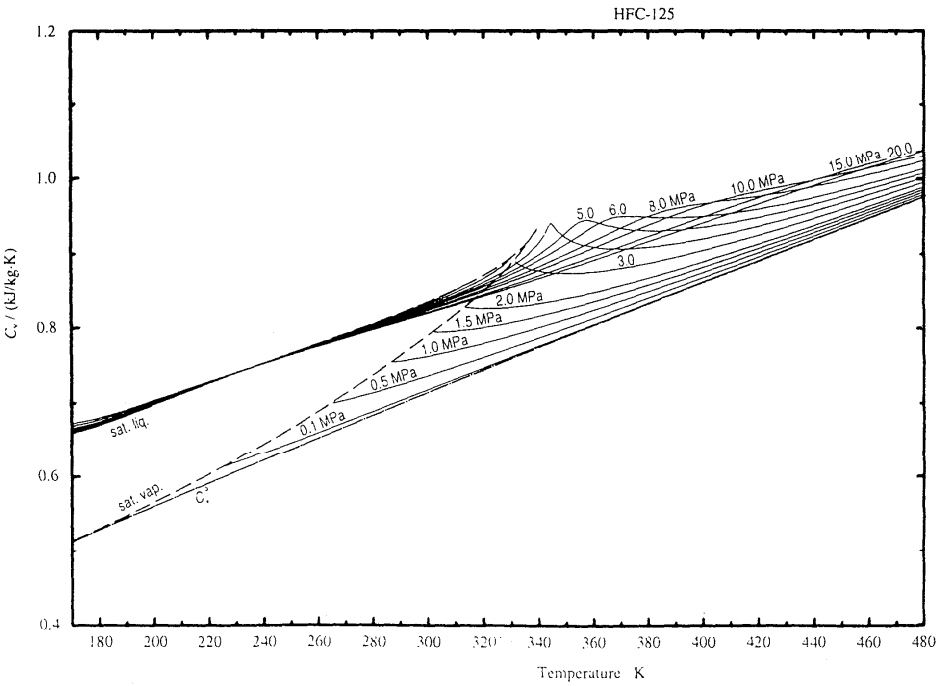

FIG. 22. Temperature dependence of isochoric heat capacity.

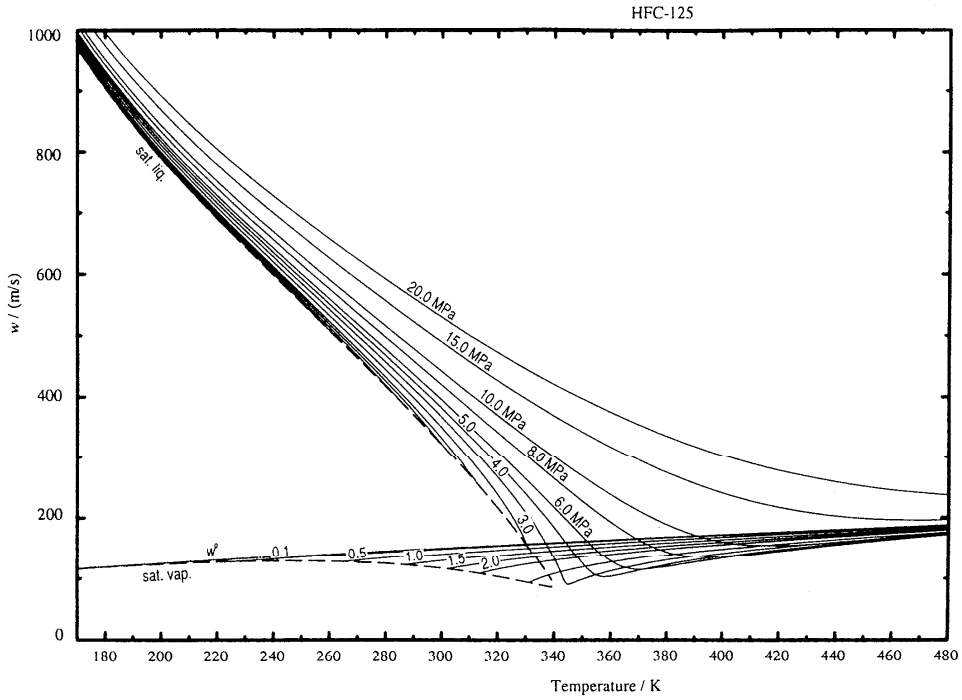

FIG. 23. Temperature dependence of speed of sound.

$$\frac{d^2u^0}{dT^2} = R[d_2 + 2d_3T], \tag{A34}$$

$$\frac{d^2s^0}{dT^2} = R\left[\frac{1-d_1}{T^2} + d_3\right]. \tag{A35}$$

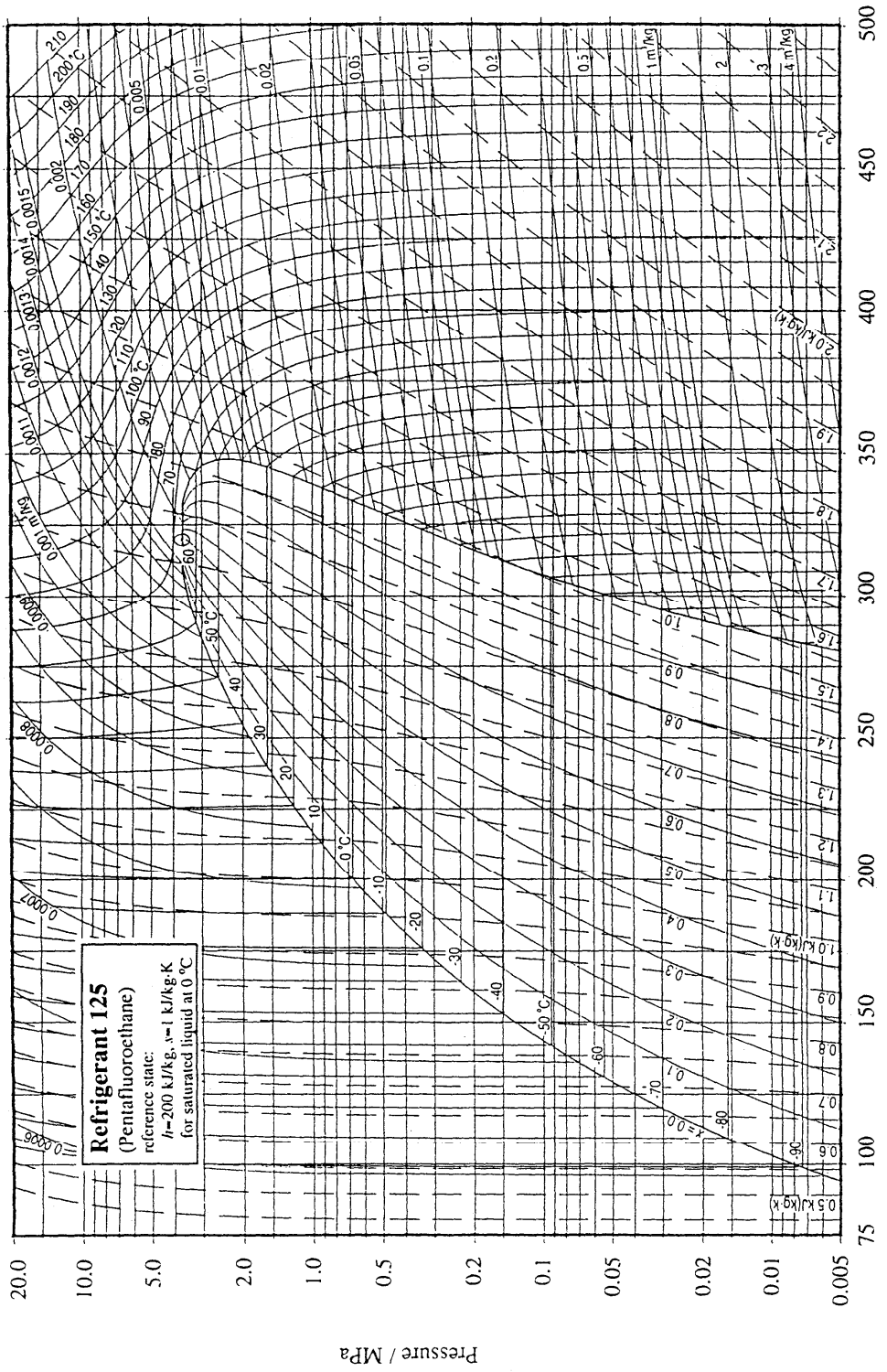

FIG. 24. Pressure-enthalpy diagram of HFC-125.

9. Appendix B: Calculated Thermodynamic Properties of HFC-125

This appendix presents tables for the properties of HFC-125 and a diagram of the thermodynamic surface on pressure-enthalpy chart (Fig. 24). The reference states for enthalpy and entropy follow the convention of the International Institute of Refrigeration, namely, $h = 200$ kJ/kg and $s = 1$ kJ/(kg K) for the saturated liquid at 0 °C.

The symbols and superscripts used in Table 12 and Table 13 are defined below.

Symbols:	t	Temperature
	P	Pressure
	ρ	Density
	h	Enthalpy
	s	Entropy
	C_p	Isobaric heat capacity
	C_v	Isochoric heat capacity
	w	Speed of sound
Superscripts:	$'$	Saturated liquid
	$''$	Saturated vapor

TABLE 12. Properties of HFC-125 along the saturation boundary

t	P	ρ'	ρ''	h'	$h''-h'$	h''	s'	s''	C'_p	C''_p	C'_v	C''_v	w'	w''
°C	kPa	kg/m^3		kJ/kg			kJ/(kg K)		kJ/(kg K)		kJ/(kg K)		m/s	
−100.63	3.0	1692.4	0.248 16	87.50	189.29	276.78	0.491 58	1.5888	1.0589	0.588 80	0.662 30	0.518 27	950.76	116.14
−100.00	3.1	1690.2	0.262 01	88.16	188.98	277.14	0.495 44	1.5869	1.0581	0.589 91	0.662 94	0.519 32	946.46	116.33
−98.00	3.8	1683.4	0.310 29	90.28	188.02	278.30	0.507 58	1.5811	1.0559	0.593 44	0.665 07	0.522 66	933.04	116.91
−96.00	4.5	1676.6	0.365 77	92.39	187.07	279.46	0.519 55	1.5755	1.0543	0.597 01	0.667 36	0.526 02	919.95	117.49
−94.00	5.3	1669.9	0.429 23	94.49	186.12	280.62	0.531 38	1.5703	1.0532	0.600 62	0.669 76	0.529 40	907.18	118.06
−92.00	6.3	1663.1	0.501 53	96.60	185.18	281.78	0.543 07	1.5653	1.0526	0.604 28	0.672 27	0.532 79	894.69	118.61
−90.00	7.4	1656.4	0.583 60	98.71	184.24	282.94	0.554 63	1.5606	1.0524	0.607 98	0.674 87	0.536 21	882.47	119.16
−88.00	8.6	1649.7	0.676 39	100.81	183.30	284.11	0.566 06	1.5561	1.0526	0.611 73	0.677 53	0.539 64	870.51	119.70
−86.00	10.0	1642.9	0.780 95	102.92	182.36	285.28	0.577 37	1.5518	1.0532	0.615 52	0.680 25	0.543 10	858.79	120.22
−84.00	11.7	1636.2	0.898 36	105.03	181.43	286.45	0.588 56	1.5477	1.0541	0.619 37	0.683 01	0.546 58	847.28	120.73
−82.00	13.5	1629.5	1.0298	107.14	180.49	287.63	0.599 65	1.5439	1.0552	0.623 28	0.685 80	0.550 08	835.99	121.24
−80.00	15.6	1622.8	1.1764	109.25	179.55	288.80	0.610 64	1.5402	1.0567	0.627 25	0.688 62	0.553 61	824.88	121.72
−78.00	17.9	1616.1	1.3396	111.36	178.61	289.97	0.621 53	1.5368	1.0584	0.631 27	0.691 46	0.557 16	813.96	122.20
−76.00	20.5	1609.3	1.5205	113.48	177.67	291.15	0.632 33	1.5335	1.0603	0.635 36	0.694 30	0.560 74	803.20	122.67
−74.00	23.4	1602.6	1.7207	115.61	176.72	292.33	0.643 04	1.5304	1.0625	0.639 52	0.697 15	0.564 34	792.60	123.12
−72.00	26.6	1595.8	1.9416	117.74	175.77	293.50	0.653 66	1.5275	1.0648	0.643 74	0.700 00	0.567 97	782.14	123.55
−70.00	30.2	1589.0	2.1846	119.87	174.81	294.68	0.664 21	1.5247	1.0674	0.648 04	0.702 85	0.571 64	771.82	123.97
−68.00	34.1	1582.2	2.4515	122.01	173.84	295.85	0.674 67	1.5221	1.0701	0.652 41	0.705 70	0.575 33	761.62	124.38
−66.00	38.5	1575.4	2.7437	124.15	172.87	297.03	0.685 06	1.5196	1.0729	0.656 86	0.708 53	0.579 05	751.55	124.77
−64.00	43.3	1568.6	3.0632	126.30	171.90	298.20	0.695 38	1.5173	1.0760	0.661 39	0.711 36	0.582 80	741.58	125.15
−62.00	48.6	1561.7	3.4115	128.46	170.91	299.37	0.705 63	1.5151	1.0792	0.666 00	0.714 17	0.586 58	731.71	125.51
−60.00	54.4	1554.8	3.7907	130.62	169.92	300.54	0.715 81	1.5130	1.0825	0.670 70	0.716 97	0.590 39	721.93	125.85
−58.00	60.7	1547.9	4.2025	132.79	168.91	301.71	0.725 92	1.5110	1.0860	0.675 49	0.719 76	0.594 24	712.25	126.18
−56.00	67.7	1540.9	4.6489	134.97	167.90	302.87	0.735 98	1.5092	1.0896	0.680 37	0.722 54	0.598 11	702.64	126.48
−54.00	75.2	1533.9	5.1321	137.16	166.88	304.04	0.745 97	1.5075	1.0933	0.685 35	0.725 30	0.602 02	693.11	126.77
−52.00	83.3	1526.9	5.6541	139.35	165.85	305.20	0.755 91	1.5058	1.0972	0.690 42	0.728 04	0.605 97	683.64	127.04
−50.00	92.2	1519.8	6.2172	141.55	164.80	306.35	0.765 79	1.5043	1.1012	0.695 60	0.730 78	0.609 94	674.24	127.30
−48.096	101.325	1513.0	6.7932	143.65	163.79	307.45	0.775 15	1.5030	1.1051	0.700 62	0.733 36	0.613 76	665.34	127.52
−48.00	101.8	1512.7	6.8235	143.76	163.74	307.50	0.775 62	1.5029	1.1053	0.700 88	0.733 49	0.613 96	664.89	127.53
−46.00	112.2	1505.5	7.4755	145.98	162.67	308.65	0.785 40	1.5015	1.1096	0.706 27	0.736 20	0.618 00	655.60	127.74
−44.00	123.3	1498.3	8.1756	148.21	161.59	309.80	0.795 13	1.5003	1.1140	0.711 78	0.738 89	0.622 08	646.35	127.93
−42.00	135.4	1491.0	8.9262	150.44	160.49	310.94	0.804 81	1.4991	1.1185	0.717 40	0.741 57	0.626 19	637.15	128.11
−40.00	148.3	1483.7	9.7301	152.69	159.38	312.07	0.814 44	1.4980	1.1231	0.723 15	0.744 24	0.630 34	627.99	128.26
−38.00	162.2	1476.3	10.590	154.94	158.26	313.20	0.824 03	1.4970	1.1279	0.729 02	0.746 90	0.634 52	618.86	128.38
−36.00	177.0	1468.9	11.508	157.21	157.12	314.32	0.833 58	1.4961	1.1328	0.735 02	0.749 55	0.638 74	609.76	128.49
−34.00	192.9	1461.4	12.489	159.48	155.96	315.44	0.843 09	1.4952	1.1379	0.741 17	0.752 19	0.642 99	600.69	128.57
−32.00	209.9	1453.8	13.533	161.77	154.78	316.55	0.852 56	1.4944	1.1431	0.747 46	0.754 82	0.647 28	591.64	128.63
−30.00	228.0	1446.2	14.646	164.06	153.59	317.66	0.861 98	1.4937	1.1484	0.753 89	0.757 45	0.651 60	582.61	128.67
−28.00	247.3	1438.5	15.830	166.37	152.38	318.75	0.871 38	1.4930	1.1539	0.760 49	0.760 08	0.655 96	573.60	128.68
−26.00	267.8	1430.7	17.088	168.69	151.16	319.85	0.880 74	1.4923	1.1595	0.767 25	0.762 70	0.660 35	564.59	128.66
−24.00	289.6	1422.9	18.424	171.02	149.91	320.93	0.890 06	1.4918	1.1654	0.774 19	0.765 31	0.664 78	555.60	128.62
−22.00	312.8	1414.9	19.842	173.36	148.64	322.00	0.899 36	1.4912	1.1714	0.781 30	0.767 93	0.669 24	546.62	128.55

TABLE 12. Properties of HFC-125 along the saturation boundary—(Continued)

t	P	ρ'	ρ''	h'	$h''-h'$	h''	s'	s''	C_p'	C_p''	C_v'	C_v''	w'	w''
°C	kPa	kg/m³			kJ/kg		kJ/(kg K)		kJ/(kg K)		kJ/(kg K)		m/s	
−20.00	337.3	1406.9	21.345	175.71	147.36	323.07	0.908 62	1.4907	1.1775	0.788 62	0.770 55	0.673 74	537.63	128.46
−18.00	363.2	1398.8	22.938	178.08	146.05	324.13	0.917 86	1.4903	1.1839	0.796 13	0.773 17	0.678 28	528.65	128.34
−16.00	390.7	1390.6	24.625	180.46	144.72	325.17	0.927 07	1.4898	1.1905	0.803 86	0.775 79	0.682 85	519.66	128.19
−14.00	419.7	1382.3	26.411	182.85	143.36	326.21	0.936 26	1.4895	1.1973	0.811 83	0.778 42	0.687 46	510.66	128.01
−12.00	450.3	1373.9	28.299	185.26	141.98	327.24	0.945 42	1.4891	1.2043	0.820 03	0.781 05	0.692 10	501.66	127.80
−10.00	482.6	1365.3	30.296	187.68	140.58	328.25	0.954 56	1.4888	1.2116	0.828 50	0.783 69	0.696 79	492.64	127.56
−8.00	516.5	1356.7	32.406	190.11	139.15	329.26	0.963 68	1.4885	1.2191	0.837 25	0.786 34	0.701 51	483.61	127.29
−6.00	552.3	1347.9	34.635	192.56	137.69	330.25	0.972 78	1.4882	1.2270	0.846 31	0.789 00	0.706 27	474.56	126.99
−4.00	589.8	1339.1	36.989	195.02	136.21	331.23	0.981 87	1.4879	1.2351	0.855 68	0.791 67	0.711 06	465.49	126.65
−2.00	629.3	1330.0	39.475	197.50	134.70	332.20	0.990 94	1.4877	1.2436	0.865 41	0.794 36	0.715 90	456.39	126.28
0.00	670.7	1320.9	42.098	200.00	133.15	333.15	1.0000	1.4875	1.2524	0.875 52	0.797 06	0.720 77	447.26	125.88
2.00	714.1	1311.6	44.867	202.51	131.58	334.09	1.0090	1.4872	1.2616	0.886 05	0.799 78	0.725 69	438.10	125.44
4.00	759.6	1302.1	47.789	205.05	129.97	335.01	1.0181	1.4870	1.2712	0.897 03	0.802 52	0.730 65	428.91	124.96
6.00	807.2	1292.5	50.873	207.59	128.32	335.92	1.0271	1.4868	1.2812	0.908 50	0.805 29	0.735 65	419.68	124.45
8.00	857.0	1282.7	54.127	210.16	126.64	336.80	1.0362	1.4866	1.2918	0.920 52	0.808 08	0.740 69	410.41	123.89
10.00	909.0	1272.7	57.562	212.75	124.92	337.67	1.0452	1.4864	1.3029	0.933 15	0.810 89	0.745 78	401.09	123.30
12.00	963.4	1262.6	61.189	215.36	123.16	338.52	1.0542	1.4861	1.3146	0.946 45	0.813 73	0.750 92	391.72	122.66
14.00	1020.1	1252.2	65.018	217.99	121.36	339.35	1.0632	1.4859	1.3270	0.960 50	0.816 61	0.756 10	382.30	121.98
16.00	1079.3	1241.6	69.064	220.64	119.51	340.16	1.0723	1.4856	1.3401	0.975 38	0.819 52	0.761 34	372.83	121.26
18.00	1141.1	1230.7	73.340	223.32	117.62	340.94	1.0813	1.4853	1.3541	0.991 21	0.822 46	0.766 63	363.29	120.49
20.00	1205.4	1219.7	77.862	226.02	115.67	341.69	1.0904	1.4850	1.3690	1.0081	0.825 45	0.771 97	353.69	119.67
22.00	1272.4	1208.3	82.647	228.75	113.67	342.42	1.0995	1.4846	1.3849	1.0262	0.828 49	0.777 38	344.02	118.80
24.00	1342.1	1196.6	87.716	231.50	111.61	343.12	1.1086	1.4842	1.4021	1.0457	0.831 57	0.782 84	334.27	117.88
26.00	1414.6	1184.7	93.089	234.28	109.50	343.78	1.1177	1.4837	1.4206	1.0668	0.834 70	0.788 37	324.44	116.91
28.00	1490.0	1172.4	98.793	237.10	107.31	344.41	1.1269	1.4832	1.4407	1.0898	0.837 90	0.793 97	314.53	115.89
30.00	1568.4	1159.7	104.86	239.95	105.05	345.00	1.1361	1.4826	1.4626	1.1150	0.841 15	0.799 65	304.52	114.81
32.00	1649.8	1146.6	111.31	242.83	102.72	345.54	1.1453	1.4819	1.4866	1.1427	0.844 48	0.805 41	294.41	113.66
34.00	1734.4	1133.0	118.19	245.75	100.29	346.04	1.1546	1.4812	1.5132	1.1735	0.847 88	0.811 25	284.20	112.46
36.00	1822.2	1119.0	125.55	248.71	97.78	346.49	1.1640	1.4803	1.5428	1.2080	0.851 37	0.817 20	273.87	111.20
38.00	1913.4	1104.4	133.43	251.72	95.16	346.88	1.1734	1.4793	1.5761	1.2470	0.854 96	0.823 24	263.42	109.87
40.00	2007.9	1089.3	141.89	254.77	92.43	347.21	1.1829	1.4781	1.6138	1.2916	0.858 65	0.829 41	252.84	108.47
42.00	2106.0	1073.4	151.01	257.89	89.58	347.46	1.1925	1.4768	1.6570	1.3431	0.862 45	0.835 70	242.11	107.01
44.00	2207.8	1056.7	160.89	261.06	86.57	347.63	1.2023	1.4753	1.7074	1.4034	0.866 39	0.842 13	231.23	105.47
46.00	2313.3	1039.2	171.62	264.30	83.41	347.71	1.2122	1.4735	1.7668	1.4753	0.870 49	0.848 73	220.18	103.87
48.00	2422.7	1020.6	183.35	267.62	80.05	347.67	1.2222	1.4715	1.8383	1.5626	0.874 75	0.855 51	208.95	102.19
50.00	2536.2	1000.8	196.27	271.03	76.47	347.51	1.2324	1.4691	1.9262	1.6708	0.879 22	0.862 50	197.51	100.44
52.00	2653.9	979.50	210.62	274.56	72.63	347.18	1.2429	1.4663	2.0376	1.8088	0.883 93	0.869 74	185.86	98.62
54.00	2776.0	956.37	226.73	278.21	68.46	346.67	1.2538	1.4630	2.1835	1.9909	0.888 92	0.877 27	173.96	96.74
56.00	2902.7	930.93	245.08	282.04	63.87	345.91	1.2650	1.4591	2.3838	2.2421	0.894 26	0.885 14	161.80	94.80
58.00	3034.3	902.42	266.39	286.09	58.75	344.84	1.2768	1.4543	2.6769	2.6101	0.900 05	0.893 45	149.34	92.83
60.00	3171.0	869.62	291.85	290.45	52.88	343.33	1.2895	1.4482	3.1466	3.1980	0.906 42	0.902 29	136.56	90.84
62.00	3313.3	830.24	323.68	295.29	45.88	341.17	1.3035	1.4404	4.0179	4.2760	0.913 60	0.911 84	123.44	88.88
64.00	3461.7	779.19	366.82	301.01	36.88	337.88	1.3199	1.4293	6.1405	6.8345	0.922 05	0.922 40	109.97	87.06
66.00	3616.9	698.77	438.49	308.99	22.90	331.89	1.3429	1.4105	17.173	19.359	0.932 86	0.934 48	96.11	85.69
66.015	3617.5	568.00	568.00	319.47	0.00	319.47	1.3738	1.3738	–	–	–	–	–	–

TABLE 13. Properties of HFC-125 in the single-phase region

t °C	ρ kg/m^3	h kJ/kg	s kJ/(kg K)	C_p kJ/(kg K)	C_v kJ/(kg K)	w m/s
			$P=50$ kPa			
Sat. liq. −61.505	1560.0	129.00	0.708 15	1.0800	0.714 87	729.28
Sat. vap. −61.505	3.5025	299.66	1.5145	0.667 16	0.587 52	125.59
−90.00	1656.5	98.72	0.554 57	1.0524	0.674 89	882.70
−80.00	1622.9	109.26	0.610 60	1.0566	0.688 63	825.07
−70.00	1589.1	119.88	0.664 18	1.0673	0.702 86	771.94
−60.00	3.4753	300.67	1.5193	0.668 95	0.589 61	126.08
−50.00	3.3059	307.42	1.5502	0.681 28	0.603 68	129.20
−40.00	3.1537	314.29	1.5804	0.694 26	0.618 02	132.20
−30.00	3.0159	321.30	1.6098	0.707 69	0.632 53	135.10
−20.00	2.8905	328.45	1.6386	0.721 47	0.647 17	137.91
−10.00	2.7756	335.73	1.6668	0.735 49	0.661 89	140.63
0.00	2.6700	343.16	1.6945	0.749 69	0.676 67	143.28
10.00	2.5725	350.73	1.7217	0.764 02	0.691 48	145.87
20.00	2.4821	358.44	1.7485	0.778 44	0.706 30	148.40
30.00	2.3980	366.30	1.7748	0.792 93	0.721 13	150.87
40.00	2.3197	374.30	1.8008	0.807 45	0.735 94	153.29
50.00	2.2464	382.45	1.8264	0.822 00	0.750 73	155.66
60.00	2.1777	390.74	1.8517	0.836 56	0.765 50	157.99
70.00	2.1131	399.18	1.8766	0.851 12	0.780 24	160.28
80.00	2.0524	407.76	1.9013	0.865 66	0.794 94	162.53
90.00	1.9951	416.49	1.9257	0.880 19	0.809 61	164.75
100.00	1.9410	425.37	1.9498	0.894 69	0.824 23	166.93
110.00	1.8897	434.38	1.9736	0.909 17	0.838 81	169.08
120.00	1.8412	443.55	1.9972	0.923 60	0.853 34	171.20
130.00	1.7951	452.86	2.0206	0.938 01	0.867 82	173.28
140.00	1.7512	462.31	2.0438	0.952 37	0.882 26	175.34
150.00	1.7095	471.90	2.0667	0.966 69	0.896 65	177.38
160.00	1.6698	481.64	2.0895	0.980 97	0.910 98	179.38
170.00	1.6318	491.52	2.1120	0.995 20	0.925 27	181.37
180.00	1.5956	501.55	2.1344	1.0094	0.939 50	183.33
190.00	1.5609	511.71	2.1566	1.0235	0.953 68	185.26
200.00	1.5278	522.02	2.1786	1.0376	0.967 81	187.18
			$P=100$ kPa			
Sat. liq. −48.365	1514.0	143.36	0.773 84	1.1046	0.733 00	666.59
Sat. vap. −48.365	6.7096	307.29	1.5031	0.699 91	0.613 22	127.49
−90.00	1656.6	98.74	0.554 51	1.0523	0.674 91	882.96
−80.00	1623.0	109.28	0.610 53	1.0566	0.688 64	825.35
−70.00	1589.2	119.89	0.664 11	1.0672	0.702 86	772.24
−60.00	1554.9	130.64	0.715 74	1.0824	0.716 98	722.23
−50.00	1519.8	141.55	0.765 78	1.1012	0.730 77	674.29
−40.00	6.4319	313.18	1.5289	0.708 31	0.624 18	130.24
−30.00	6.1328	320.32	1.5588	0.719 39	0.637 68	133.38
−20.00	5.8638	327.57	1.5881	0.731 31	0.651 52	136.39
−10.00	5.6200	334.95	1.6166	0.743 85	0.665 59	139.29
0.00	5.3975	342.45	1.6446	0.756 85	0.679 83	142.08
10.00	5.1934	350.09	1.6721	0.770 20	0.694 21	144.79
20.00	5.0053	357.86	1.6990	0.783 81	0.708 66	147.43
30.00	4.8312	365.76	1.7256	0.797 62	0.723 18	149.99
40.00	4.6696	373.81	1.7517	0.811 58	0.737 74	152.49
50.00	4.5189	382.00	1.7774	0.825 65	0.752 31	154.94
60.00	4.3781	390.32	1.8028	0.839 80	0.766 90	157.33
70.00	4.2462	398.79	1.8278	0.854 00	0.781 48	159.67
80.00	4.1222	407.40	1.8526	0.868 25	0.796 04	161.97
90.00	4.0056	416.16	1.8770	0.882 51	0.810 59	164.23
100.00	3.8955	425.05	1.9012	0.896 79	0.825 11	166.45

TABLE 13. Properties of HFC-125 in the single-phase region—Continued

t °C	ρ kg/m^3	h kJ/kg	s kJ/(kg K)	C_p kJ/(kg K)	C_v kJ/(kg K)	w m/s
			$P = 100$ kPa			
110.00	3.7915	434.09	1.9251	0.911 06	0.839 60	168.64
120.00	3.6931	443.27	1.9487	0.925 32	0.854 05	170.79
130.00	3.5997	452.60	1.9721	0.939 57	0.868 47	172.90
140.00	3.5110	462.07	1.9953	0.953 80	0.882 84	174.99
150.00	3.4267	471.68	2.0183	0.968 00	0.897 17	177.05
160.00	3.3464	481.43	2.0411	0.982 17	0.911 46	179.07
170.00	3.2699	491.32	2.0637	0.996 30	0.925 71	181.08
180.00	3.1968	501.35	2.0861	1.0104	0.939 90	183.06
190.00	3.1270	511.53	2.1083	1.0245	0.954 05	185.01
200.00	3.0602	521.84	2.1303	1.0385	0.968 14	186.94
			$P = 101.325$ kPa			
Sat. liq. −48.096	1513.0	143.65	0.775 15	1.1051	0.733 36	665.34
Sat. vap. −48.096	6.7932	307.45	1.5030	0.700 62	0.613 76	127.52
−90.00	1656.6	98.74	0.554 51	1.0523	0.674 91	882.97
−80.00	1623.0	109.28	0.610 53	1.0566	0.688 64	825.36
−70.00	1589.2	119.89	0.664 11	1.0672	0.702 86	772.24
−60.00	1555.0	130.64	0.715 74	1.0824	0.716 98	722.24
−50.00	1519.8	141.55	0.765 78	1.1012	0.730 77	674.30
−40.00	6.5205	313.15	1.5279	0.708 70	0.624 35	130.19
−30.00	6.2169	320.29	1.5578	0.719 71	0.637 82	133.34
−20.00	5.9438	327.55	1.5871	0.731 58	0.651 63	136.35
−10.00	5.6963	334.93	1.6157	0.744 08	0.665 69	139.25
0.00	5.4706	342.43	1.6437	0.757 05	0.679 92	142.05
10.00	5.2635	350.07	1.6711	0.770 37	0.694 28	144.77
20.00	5.0728	357.84	1.6981	0.783 96	0.708 73	147.40
30.00	4.8962	365.75	1.7246	0.797 75	0.723 24	149.97
40.00	4.7323	373.80	1.7507	0.811 69	0.737 79	152.47
50.00	4.5795	381.98	1.7765	0.825 75	0.752 36	154.92
60.00	4.4367	390.31	1.8018	0.839 89	0.766 93	157.31
70.00	4.3030	398.78	1.8269	0.854 08	0.781 51	159.66
80.00	4.1773	407.39	1.8516	0.868 32	0.796 07	161.96
90.00	4.0591	416.15	1.8761	0.882 57	0.810 61	164.22
100.00	3.9475	425.05	1.9002	0.896 84	0.825 13	166.44
110.00	3.8421	434.09	1.9241	0.911 11	0.839 62	168.62
120.00	3.7423	443.27	1.9478	0.925 37	0.854 07	170.77
130.00	3.6477	452.59	1.9712	0.939 61	0.868 48	172.89
140.00	3.5578	462.06	1.9944	0.953 84	0.882 86	174.98
150.00	3.4723	471.67	2.0174	0.968 03	0.897 19	177.04
160.00	3.3910	481.42	2.0402	0.982 20	0.911 48	179.07
170.00	3.3134	491.31	2.0628	0.996 33	0.925 72	181.07
180.00	3.2393	501.35	2.0851	1.0104	0.939 91	183.05
190.00	3.1685	511.52	2.1074	1.0245	0.954 05	185.00
200.00	3.1008	521.84	2.1294	1.0385	0.968 15	186.93
			$P = 150$ kPa			
Sat. liq. −39.746	1482.8	152.97	0.815 66	1.1237	0.744 58	626.83
Sat. vap. −39.746	9.8360	312.21	1.4979	0.723 88	0.630 87	128.27
−90.00	1656.7	98.76	0.554 45	1.0523	0.674 93	883.23
−80.00	1623.1	109.30	0.610 47	1.0565	0.688 66	825.63
−70.00	1589.3	119.91	0.664 05	1.0672	0.702 87	772.53
−60.00	1555.1	130.66	0.715 67	1.0823	0.716 98	722.55
−50.00	1520.0	141.57	0.765 70	1.1011	0.730 77	674.64
−40.00	1483.7	152.69	0.814 44	1.1231	0.744 24	628.00
−30.00	9.3606	319.31	1.5277	0.732 00	0.642 99	131.60
−20.00	8.9268	326.68	1.5574	0.741 80	0.655 97	134.83

TABLE 13. Properties of HFC-125 in the single-phase region—Continued

t °C	ρ kg/m^3	h kJ/kg	s kJ/(kg K)	C_p kJ/(kg K)	C_v kJ/(kg K)	w m/s
			$P=150$ kPa			
−10.00	8.5378	334.15	1.5863	0.752 68	0.669 36	137.91
0.00	8.1858	341.73	1.6146	0.764 36	0.683 05	140.86
10.00	7.8653	349.44	1.6423	0.776 64	0.696 97	143.70
20.00	7.5715	357.27	1.6695	0.789 38	0.711 05	146.44
30.00	7.3010	365.22	1.6962	0.802 46	0.725 26	149.10
40.00	7.0508	373.32	1.7224	0.815 82	0.739 55	151.69
50.00	6.8184	381.54	1.7483	0.829 39	0.753 91	154.20
60.00	6.6019	389.90	1.7738	0.843 11	0.768 30	156.66
70.00	6.3995	398.40	1.7989	0.856 95	0.782 72	159.06
80.00	6.2099	407.04	1.8237	0.870 88	0.797 15	161.41
90.00	6.0317	415.82	1.8483	0.884 87	0.811 57	163.71
100.00	5.8639	424.74	1.8725	0.898 91	0.825 99	165.97
110.00	5.7055	433.80	1.8964	0.912 98	0.840 39	168.19
120.00	5.5558	443.00	1.9201	0.927 06	0.854 76	170.37
130.00	5.4140	452.34	1.9436	0.941 15	0.869 11	172.52
140.00	5.2795	461.82	1.9668	0.955 24	0.883 42	174.63
150.00	5.1517	471.45	1.9898	0.969 32	0.897 70	176.71
160.00	5.0301	481.21	2.0126	0.983 38	0.911 94	178.77
170.00	4.9142	491.11	2.0353	0.997 42	0.926 14	180.79
180.00	4.8037	501.16	2.0577	1.0114	0.940 30	182.79
190.00	4.6981	511.34	2.0799	1.0254	0.954 41	184.76
200.00	4.5972	521.67	2.1019	1.0394	0.968 48	186.70
			$P=200$ kPa			
Sat. liq. −33.150	1458.2	160.45	0.847 12	1.1401	0.753 31	596.84
Sat. vap. −33.150	12.925	315.91	1.4949	0.743 82	0.644 81	128.60
−90.00	1656.8	98.78	0.554 39	1.0523	0.674 95	883.49
−80.00	1623.2	109.32	0.610 41	1.0565	0.688 67	825.91
−70.00	1589.5	119.93	0.663 98	1.0671	0.702 88	772.83
−60.00	1555.2	130.67	0.715 60	1.0822	0.716 98	722.87
−50.00	1520.2	141.59	0.765 63	1.1009	0.730 77	674.98
−40.00	1483.9	152.70	0.814 36	1.1229	0.744 23	628.38
−30.00	12.711	318.26	1.5046	0.745 69	0.648 46	129.74
−20.00	12.087	325.75	1.5348	0.753 02	0.660 54	133.21
−10.00	11.534	333.33	1.5641	0.762 02	0.673 21	136.49
0.00	11.039	341.00	1.5927	0.772 23	0.686 32	139.60
10.00	10.591	348.77	1.6207	0.783 35	0.699 77	142.58
20.00	10.183	356.67	1.6481	0.795 14	0.713 47	145.44
30.00	9.8088	364.68	1.6750	0.807 46	0.727 36	148.20
40.00	9.4644	372.82	1.7014	0.820 18	0.741 38	150.87
50.00	9.1457	381.08	1.7274	0.833 21	0.755 51	153.46
60.00	8.8497	389.48	1.7529	0.846 49	0.769 72	155.98
70.00	8.5737	398.01	1.7782	0.859 95	0.783 97	158.44
80.00	8.3157	406.68	1.8031	0.873 55	0.798 26	160.84
90.00	8.0737	415.48	1.8277	0.887 26	0.812 56	163.19
100.00	7.8462	424.43	1.8519	0.901 06	0.826 87	165.49
110.00	7.6319	433.51	1.8760	0.914 92	0.841 18	167.75
120.00	7.4295	442.72	1.8997	0.928 82	0.855 48	169.96
130.00	7.2381	452.08	1.9232	0.942 75	0.869 75	172.14
140.00	7.0567	461.58	1.9465	0.956 70	0.884 01	174.28
150.00	6.8845	471.22	1.9695	0.970 65	0.898 23	176.38
160.00	6.7207	480.99	1.9924	0.984 60	0.912 42	178.46
170.00	6.5649	490.91	2.0150	0.998 54	0.926 58	180.50
180.00	6.4163	500.96	2.0374	1.0125	0.940 70	182.52
190.00	6.2744	511.16	2.0597	1.0264	0.954 78	184.51

TABLE 13. Properties of HFC-125 in the single-phase region—Continued

t °C	ρ kg/m³	h kJ/kg	s kJ/(kg K)	C_p kJ/(kg K)	C_v kJ/(kg K)	w m/s
			$P=200$ kPa			
200.00	6.1389	521.49	2.0818	1.0402	0.968 81	186.47
			$P=300$ kPa			
Sat. liq. −23.089	1419.3	172.08	0.894 30	1.1681	0.766 51	551.51
Sat. vap. −23.089	19.060	321.42	1.4915	0.777 41	0.666 81	128.59
−90.00	1657.0	98.82	0.554 27	1.0522	0.674 99	884.02
−80.00	1623.4	109.35	0.610 28	1.0564	0.688 70	826.47
−70.00	1589.7	119.97	0.663 84	1.0669	0.702 90	773.43
−60.00	1555.5	130.71	0.715 46	1.0820	0.716 99	723.51
−50.00	1520.5	141.62	0.765 47	1.1006	0.730 77	675.68
−40.00	1484.3	152.73	0.814 19	1.1226	0.744 22	629.13
−30.00	1446.5	164.08	0.861 85	1.1481	0.757 43	583.21
−20.00	18.738	323.82	1.5010	0.778 14	0.670 05	129.80
−10.00	17.790	331.62	1.5313	0.782 54	0.681 17	133.52
0.00	16.956	339.48	1.5606	0.789 27	0.693 06	136.99
10.00	16.215	347.41	1.5891	0.797 69	0.705 51	140.27
20.00	15.549	355.44	1.6169	0.807 36	0.718 40	143.38
30.00	14.945	363.56	1.6442	0.817 97	0.731 62	146.35
40.00	14.394	371.80	1.6709	0.829 29	0.745 10	149.20
50.00	13.887	380.15	1.6972	0.841 17	0.758 76	151.95
60.00	13.420	388.62	1.7230	0.853 48	0.772 57	154.61
70.00	12.987	397.22	1.7484	0.866 13	0.786 49	157.19
80.00	12.583	405.95	1.7735	0.879 05	0.800 49	159.70
90.00	12.207	414.80	1.7982	0.892 17	0.814 55	162.14
100.00	11.854	423.79	1.8226	0.905 47	0.828 65	164.52
110.00	11.523	432.91	1.8468	0.918 89	0.842 78	166.86
120.00	11.210	442.17	1.8706	0.932 41	0.856 91	169.14
130.00	10.916	451.56	1.8942	0.946 00	0.871 05	171.37
140.00	10.638	461.09	1.9175	0.959 66	0.885 18	173.57
150.00	10.374	470.75	1.9407	0.973 35	0.899 29	175.72
160.00	10.123	480.56	1.9636	0.987 07	0.913 39	177.84
170.00	9.8853	490.50	1.9862	1.0008	0.927 46	179.93
180.00	9.6586	500.57	2.0087	1.0145	0.941 50	181.98
190.00	9.4426	510.79	2.0310	1.0283	0.955 51	184.00
200.00	9.2363	521.14	2.0531	1.0420	0.969 48	186.00
			$P=400$ kPa			
Sat. liq. −15.346	1387.9	181.24	0.930 08	1.1927	0.776 65	516.72
Sat. vap. −15.346	25.198	325.51	1.4897	0.806 44	0.684 35	128.13
−90.00	1657.2	98.85	0.554 15	1.0521	0.675 03	884.54
−80.00	1623.7	109.39	0.610 15	1.0562	0.688 73	827.03
−70.00	1590.0	120.00	0.663 71	1.0668	0.702 91	774.02
−60.00	1555.8	130.74	0.715 31	1.0818	0.717 00	724.15
−50.00	1520.8	141.65	0.765 32	1.1004	0.730 76	676.37
−40.00	1484.7	152.76	0.814 02	1.1222	0.744 20	629.89
−30.00	1447.0	164.10	0.861 67	1.1476	0.757 41	584.04
−20.00	1407.2	175.72	0.908 49	1.1771	0.770 52	538.21
−10.00	24.445	329.82	1.5063	0.806 08	0.689 53	130.35
0.00	23.190	337.89	1.5364	0.808 37	0.700 06	134.25
10.00	22.094	346.00	1.5655	0.813 48	0.711 44	137.86
20.00	21.123	354.17	1.5939	0.820 61	0.723 47	141.25
30.00	20.253	362.42	1.6215	0.829 23	0.735 99	144.45
40.00	19.467	370.76	1.6486	0.838 97	0.748 88	147.50
50.00	18.751	379.20	1.6751	0.849 56	0.762 06	150.41
60.00	18.094	387.75	1.7012	0.860 81	0.775 47	153.22
70.00	17.489	396.42	1.7268	0.872 57	0.789 04	155.92

TABLE 13. Properties of HFC-125 in the single-phase region—Continued

t °C	ρ kg/m^3	h kJ/kg	s kJ/(kg K)	C_p kJ/(kg K)	C_v kJ/(kg K)	w m/s
			$P=400$ kPa			
80.00	16.928	405.20	1.7521	0.884 75	0.802 75	158.54
90.00	16.407	414.11	1.7769	0.897 25	0.816 56	161.08
100.00	15.920	423.15	1.8015	0.910 00	0.830 44	163.55
110.00	15.465	432.31	1.8257	0.922 96	0.844 38	165.96
120.00	15.037	441.61	1.8497	0.936 08	0.858 35	168.31
130.00	14.634	451.04	1.8733	0.949 33	0.872 35	170.61
140.00	14.254	460.60	1.8968	0.962 68	0.886 35	172.86
150.00	13.895	470.29	1.9199	0.976 10	0.900 36	175.06
160.00	13.554	480.12	1.9429	0.989 59	0.914 35	177.23
170.00	13.231	490.08	1.9656	1.0031	0.928 34	179.36
180.00	12.924	500.18	1.9882	1.0167	0.942 30	181.45
190.00	12.631	510.41	2.0105	1.0302	0.956 25	183.51
200.00	12.353	520.79	2.0327	1.0438	0.970 16	185.53
			$P=500$ kPa			
Sat. liq. −8.960	1360.9	188.94	0.959 31	1.2155	0.785 07	487.95
Sat. vap. −8.960	31.379	328.78	1.4886	0.833 02	0.699 24	127.43
−90.00	1657.4	98.89	0.554 02	1.0520	0.675 07	885.07
−80.00	1623.9	109.43	0.610 03	1.0561	0.688 75	827.59
−70.00	1590.2	120.04	0.663 58	1.0666	0.702 93	774.62
−60.00	1556.1	130.77	0.715 17	1.0816	0.717 00	724.78
−50.00	1521.2	141.68	0.765 17	1.1001	0.730 76	677.06
−40.00	1485.1	152.79	0.813 85	1.1219	0.744 19	630.64
−30.00	1447.4	164.13	0.861 48	1.1471	0.757 38	584.87
−20.00	1407.8	175.74	0.908 29	1.1765	0.770 48	539.14
−10.00	1365.4	187.68	0.954 52	1.2114	0.783 68	492.83
0.00	29.790	336.23	1.5163	0.830 06	0.707 38	131.33
10.00	28.260	344.53	1.5462	0.831 02	0.717 59	135.33
20.00	26.928	352.86	1.5751	0.835 09	0.728 69	139.02
30.00	25.750	361.24	1.6032	0.841 37	0.740 46	142.48
40.00	24.697	369.69	1.6306	0.849 29	0.752 75	145.74
50.00	23.745	378.23	1.6575	0.858 43	0.765 42	148.84
60.00	22.879	386.86	1.6838	0.868 50	0.778 41	151.80
70.00	22.086	395.60	1.7096	0.879 30	0.791 63	154.63
80.00	21.354	404.45	1.7350	0.890 67	0.805 04	157.37
90.00	20.677	413.41	1.7601	0.902 50	0.818 59	160.01
100.00	20.048	422.50	1.7848	0.914 68	0.832 25	162.57
110.00	19.460	431.71	1.8091	0.927 15	0.846 00	165.06
120.00	18.910	441.04	1.8332	0.939 84	0.859 80	167.48
130.00	18.394	450.51	1.8569	0.952 73	0.873 65	169.84
140.00	17.908	460.10	1.8804	0.965 76	0.887 53	172.15
150.00	17.449	469.82	1.9037	0.978 91	0.901 42	174.41
160.00	17.015	479.68	1.9267	0.992 14	0.915 32	176.62
170.00	16.603	489.66	1.9495	1.0055	0.929 22	178.79
180.00	16.213	499.79	1.9721	1.0188	0.943 11	180.92
190.00	15.841	510.04	1.9945	1.0322	0.956 98	183.01
200.00	15.488	520.43	2.0167	1.0456	0.970 83	185.07
			$P=600$ kPa			
Sat. liq. −3.475	1336.7	195.67	0.984 25	1.2373	0.792 38	463.10
Sat. vap. −3.475	37.629	331.49	1.4879	0.858 20	0.712 33	126.56
−90.00	1657.6	98.93	0.553 90	1.0520	0.675 11	885.60
−80.00	1624.1	109.46	0.609 90	1.0560	0.688 78	828.15
−70.00	1590.5	120.07	0.663 44	1.0665	0.702 95	775.21
−60.00	1556.4	130.81	0.715 03	1.0814	0.717 01	725.42
−50.00	1521.5	141.71	0.765 01	1.0998	0.730 76	677.74

TABLE 13. Properties of HFC-125 in the single-phase region—Continued

t °C	ρ kg/m^3	h kJ/kg	s kJ/(kg K)	C_p kJ/(kg K)	C_v kJ/(kg K)	w m/s
			$P=600$ kPa			
−40.00	1485.4	152.82	0.813 69	1.1215	0.744 17	631.39
−30.00	1447.9	164.15	0.861 30	1.1466	0.757 35	585.69
−20.00	1408.3	175.76	0.908 08	1.1759	0.770 44	540.06
−10.00	1366.1	187.69	0.954 28	1.2106	0.783 62	493.87
0.00	36.821	334.46	1.4988	0.855 14	0.715 07	128.22
10.00	34.756	342.99	1.5295	0.850 73	0.723 99	132.66
20.00	32.992	351.49	1.5590	0.851 02	0.734 08	136.71
30.00	31.454	360.02	1.5876	0.854 54	0.745 05	140.45
40.00	30.095	368.59	1.6154	0.860 34	0.756 69	143.94
50.00	28.879	377.23	1.6426	0.867 84	0.768 84	147.23
60.00	27.781	385.95	1.6692	0.876 60	0.781 39	150.35
70.00	26.781	394.77	1.6952	0.886 34	0.794 25	153.33
80.00	25.865	403.68	1.7208	0.896 84	0.807 35	156.18
90.00	25.020	412.71	1.7460	0.907 93	0.820 63	158.93
100.00	24.238	421.84	1.7709	0.919 50	0.834 07	161.58
110.00	23.511	431.10	1.7953	0.931 45	0.847 62	164.15
120.00	22.832	440.47	1.8195	0.943 71	0.861 26	166.64
130.00	22.196	449.97	1.8433	0.956 21	0.874 96	169.07
140.00	21.598	459.60	1.8669	0.968 91	0.888 71	171.44
150.00	21.035	469.35	1.8903	0.981 76	0.902 49	173.75
160.00	20.504	479.23	1.9133	0.994 75	0.916 30	176.01
170.00	20.001	489.25	1.9362	1.0078	0.930 11	178.22
180.00	19.525	499.39	1.9588	1.0210	0.943 92	180.39
190.00	19.072	509.67	1.9813	1.0342	0.957 72	182.52
200.00	18.642	520.07	2.0035	1.0475	0.971 51	184.62
			$P=700$ kPa			
Sat. liq. 1.361	1314.6	201.71	1.0062	1.2586	0.798 91	441.03
Sat. vap. 1.361	43.966	333.79	1.4873	0.882 64	0.724 12	125.58
−90.00	1657.8	98.97	0.553 78	1.0519	0.675 15	886.12
−80.00	1624.3	109.50	0.609 77	1.0559	0.688 81	828.70
−70.00	1590.7	120.11	0.663 31	1.0663	0.702 96	775.80
−60.00	1556.7	130.84	0.714 89	1.0812	0.717 02	726.05
−50.00	1521.8	141.74	0.764 86	1.0996	0.730 75	678.43
−40.00	1485.8	152.84	0.813 52	1.1212	0.744 16	632.13
−30.00	1448.3	164.18	0.861 12	1.1462	0.757 33	586.51
−20.00	1408.8	175.78	0.907 88	1.1752	0.770 40	540.97
−10.00	1366.7	187.70	0.954 05	1.2097	0.783 56	494.91
0.00	1321.1	200.00	0.999 92	1.2520	0.797 04	447.61
10.00	41.633	341.37	1.5145	0.873 19	0.730 67	129.84
20.00	39.346	350.08	1.5447	0.868 74	0.739 66	134.29
30.00	37.387	358.76	1.5738	0.868 90	0.749 78	138.34
40.00	35.678	367.46	1.6021	0.872 24	0.760 73	142.08
50.00	34.164	376.21	1.6296	0.877 85	0.772 33	145.58
60.00	32.807	385.03	1.6565	0.885 14	0.784 42	148.87
70.00	31.581	393.92	1.6828	0.893 71	0.796 90	152.00
80.00	30.464	402.90	1.7086	0.903 26	0.809 68	154.98
90.00	29.439	411.99	1.7339	0.913 57	0.822 70	157.84
100.00	28.494	421.18	1.7589	0.924 48	0.835 91	160.58
110.00	27.618	430.48	1.7835	0.935 88	0.849 26	163.24
120.00	26.802	439.90	1.8078	0.947 67	0.862 73	165.81
130.00	26.041	449.43	1.8317	0.959 77	0.876 28	168.30
140.00	25.327	459.09	1.8554	0.972 12	0.889 90	170.73
150.00	24.656	468.88	1.8788	0.984 67	0.903 57	173.09
160.00	24.023	478.79	1.9019	0.997 40	0.917 27	175.40

TABLE 13. Properties of HFC-125 in the single-phase region—Continued

t °C	ρ kg/m^3	h kJ/kg	s kJ/(kg K)	C_p kJ/(kg K)	C_v kJ/(kg K)	w m/s
			$P=700$ kPa			
170.00	23.426	488.83	1.9248	1.0102	0.930 99	177.66
180.00	22.861	498.99	1.9475	1.0232	0.944 72	179.87
190.00	22.324	509.29	1.9700	1.0363	0.958 46	182.04
200.00	21.815	519.72	1.9923	1.0494	0.972 18	184.16
			$P=800$ kPa			
Sat. liq. 5.705	1293.9	207.22	1.0258	1.2797	0.804 88	421.05
Sat. vap. 5.705	50.407	335.78	1.4868	0.906 77	0.734 91	124.53
−90.00	1658.0	99.01	0.553 66	1.0518	0.675 19	886.64
−80.00	1624.6	109.54	0.609 64	1.0558	0.688 84	829.26
−70.00	1591.0	120.14	0.663 18	1.0662	0.702 98	776.40
−60.00	1557.0	130.88	0.714 74	1.0810	0.717 02	726.69
−50.00	1522.1	141.77	0.764 71	1.0993	0.730 75	679.11
−40.00	1486.2	152.87	0.813 36	1.1208	0.744 15	632.88
−30.00	1448.7	164.20	0.860 93	1.1457	0.757 30	587.33
−20.00	1409.3	175.80	0.907 67	1.1746	0.770 36	541.89
−10.00	1367.3	187.71	0.953 82	1.2088	0.783 50	495.95
0.00	1321.9	200.00	0.999 65	1.2507	0.796 95	448.81
10.00	48.959	339.66	1.5006	0.899 23	0.737 68	126.83
20.00	46.033	348.59	1.5316	0.888 64	0.745 45	131.74
30.00	43.575	357.46	1.5614	0.884 68	0.754 64	136.14
40.00	41.461	366.30	1.5901	0.885 10	0.764 87	140.16
50.00	39.610	375.17	1.6180	0.888 55	0.775 88	143.88
60.00	37.967	384.08	1.6451	0.894 18	0.787 50	147.37
70.00	36.492	393.06	1.6717	0.901 45	0.799 59	150.65
80.00	35.156	402.11	1.6977	0.909 95	0.812 04	153.76
90.00	33.936	411.26	1.7232	0.919 42	0.824 78	156.73
100.00	32.817	420.50	1.7483	0.929 63	0.837 76	159.58
110.00	31.783	429.85	1.7731	0.940 45	0.850 91	162.32
120.00	30.823	439.32	1.7974	0.951 74	0.864 20	164.97
130.00	29.929	448.89	1.8215	0.963 41	0.877 61	167.53
140.00	29.094	458.58	1.8452	0.975 40	0.891 09	170.02
150.00	28.310	468.40	1.8687	0.987 64	0.904 65	172.44
160.00	27.573	478.34	1.8919	1.0001	0.918 25	174.80
170.00	26.877	488.40	1.9149	1.0127	0.931 88	177.10
180.00	26.220	498.59	1.9376	1.0255	0.945 53	179.35
190.00	25.598	508.91	1.9601	1.0383	0.959 19	181.55
200.00	25.007	519.36	1.9825	1.0513	0.972 86	183.71
			$P=900$ kPa			
Sat. liq. 9.660	1274.5	212.31	1.0436	1.3010	0.810 41	402.68
Sat. vap. 9.660	56.965	337.53	1.4864	0.930 96	0.744 91	123.40
−90.00	1658.2	99.04	0.553 54	1.0517	0.675 23	887.17
−80.00	1624.8	109.58	0.609 52	1.0557	0.688 86	829.81
−70.00	1591.2	120.18	0.663 04	1.0660	0.703 00	776.99
−60.00	1557.2	130.91	0.714 60	1.0808	0.717 03	727.32
−50.00	1522.5	141.81	0.764 56	1.0990	0.730 75	679.80
−40.00	1486.6	152.90	0.813 19	1.1205	0.744 13	633.62
−30.00	1449.2	164.23	0.860 75	1.1452	0.757 28	588.15
−20.00	1409.8	175.82	0.907 47	1.1740	0.770 32	542.80
−10.00	1368.0	187.72	0.953 58	1.2079	0.783 44	496.98
0.00	1322.7	200.00	0.999 38	1.2494	0.796 86	450.00
10.00	56.823	337.84	1.4875	0.930 08	0.745 09	123.60
20.00	53.103	347.04	1.5194	0.911 29	0.751 50	129.05
30.00	50.049	356.10	1.5498	0.902 18	0.759 67	133.85
40.00	47.465	365.10	1.5791	0.899 09	0.769 12	138.18

TABLE 13. Properties of HFC-125 in the single-phase region—Continued

	t °C	ρ kg/m^3	h kJ/kg	s kJ/(kg K)	C_p kJ/(kg K)	C_v kJ/(kg K)	w m/s
				$P = 900$ kPa			
	50.00	45.232	374.10	1.6073	0.900 02	0.779 52	142.15
	60.00	43.268	383.11	1.6348	0.903 78	0.790 64	145.83
	70.00	41.519	392.18	1.6616	0.909 59	0.802 31	149.27
	80.00	39.945	401.31	1.6878	0.916 95	0.814 43	152.53
	90.00	38.516	410.52	1.7136	0.925 50	0.826 89	155.62
	100.00	37.209	419.82	1.7388	0.934 96	0.839 62	158.57
	110.00	36.007	429.22	1.7637	0.945 15	0.852 57	161.40
	120.00	34.896	438.73	1.7882	0.955 92	0.865 68	164.13
	130.00	33.863	448.34	1.8123	0.967 15	0.878 94	166.76
	140.00	32.900	458.07	1.8362	0.978 76	0.892 29	169.31
	150.00	31.999	467.92	1.8597	0.990 67	0.905 73	171.79
	160.00	31.153	477.89	1.8830	1.0028	0.919 23	174.20
	170.00	30.356	487.98	1.9060	1.0152	0.932 77	176.54
	180.00	29.604	498.19	1.9288	1.0277	0.946 34	178.84
	190.00	28.892	508.53	1.9514	1.0404	0.959 94	181.08
	200.00	28.218	519.00	1.9738	1.0532	0.973 54	183.27
				$P = 1000$ kPa			
Sat. liq.	13.300	1255.8	217.07	1.0601	1.3226	0.815 60	385.61
Sat. vap.	13.300	63.654	339.06	1.4860	0.955 49	0.754 28	122.22
	−90.00	1658.4	99.08	0.553 41	1.0517	0.675 27	887.69
	−80.00	1625.0	109.61	0.609 39	1.0556	0.688 89	830.37
	−70.00	1591.5	120.22	0.662 91	1.0658	0.703 01	777.58
	−60.00	1557.5	130.94	0.714 46	1.0806	0.717 04	727.95
	−50.00	1522.8	141.84	0.764 40	1.0988	0.730 74	680.48
	−40.00	1486.9	152.93	0.813 02	1.1201	0.744 12	634.37
	−30.00	1449.6	164.25	0.860 57	1.1448	0.757 25	588.97
	−20.00	1410.4	175.84	0.907 26	1.1734	0.770 28	543.71
	−10.00	1368.6	187.74	0.953 35	1.2071	0.783 38	498.00
	0.00	1323.4	200.00	0.999 11	1.2482	0.796 78	451.19
	10.00	1273.6	212.74	1.0449	1.3011	0.810 77	402.37
	20.00	60.620	345.40	1.5078	0.937 50	0.757 83	126.20
	30.00	56.846	354.69	1.5390	0.921 78	0.764 88	131.46
	40.00	53.714	363.86	1.5688	0.914 41	0.773 48	136.13
	50.00	51.044	372.99	1.5975	0.912 38	0.783 23	140.36
	60.00	48.721	382.12	1.6253	0.913 99	0.793 83	144.26
	70.00	46.670	391.28	1.6524	0.918 18	0.805 08	147.88
	80.00	44.836	400.49	1.6788	0.924 28	0.816 85	151.28
	90.00	43.181	409.77	1.7048	0.931 82	0.829 02	154.50
	100.00	41.674	419.13	1.7302	0.940 47	0.841 50	157.56
	110.00	40.294	428.58	1.7552	0.950 00	0.854 24	160.48
	120.00	39.022	438.14	1.7798	0.960 21	0.867 18	163.29
	130.00	37.843	447.79	1.8040	0.970 98	0.880 27	165.99
	140.00	36.747	457.56	1.8280	0.982 19	0.893 50	168.61
	150.00	35.723	467.44	1.8516	0.993 76	0.906 82	171.14
	160.00	34.763	477.43	1.8749	1.0056	0.920 21	173.60
	170.00	33.861	487.55	1.8980	1.0177	0.933 66	175.99
	180.00	33.012	497.79	1.9209	1.0300	0.947 16	178.33
	190.00	32.209	508.15	1.9435	1.0425	0.960 68	180.60
	200.00	31.448	518.64	1.9659	1.0551	0.974 21	182.83
				$P = 2000$ kPa			
Sat. liq.	39.835	1090.5	254.52	1.1821	1.6105	0.858 34	253.72
Sat. vap.	39.835	141.17	347.19	1.4782	1.2876	0.828 89	108.59
	−90.00	1660.3	99.46	0.552 20	1.0509	0.675 68	892.88

TABLE 13. Properties of HFC-125 in the single-phase region—Continued

t °C	ρ kg/m^3	h kJ/kg	s kJ/(kg K)	C_p kJ/(kg K)	C_v kJ/(kg K)	w m/s
			$P=2000$ kPa			
−80.00	1627.2	109.98	0.608 13	1.0545	0.689 18	835.86
−70.00	1594.0	120.57	0.661 59	1.0644	0.703 19	783.42
−60.00	1560.3	131.29	0.713 06	1.0786	0.717 12	734.21
−50.00	1526.0	142.16	0.762 90	1.0962	0.730 73	687.22
−40.00	1490.6	153.22	0.811 39	1.1168	0.744 00	641.69
−30.00	1453.9	164.50	0.858 77	1.1404	0.757 02	597.00
−20.00	1415.4	176.04	0.905 26	1.1675	0.769 91	552.62
−10.00	1374.7	187.87	0.951 08	1.1990	0.782 83	508.04
0.00	1330.9	200.04	0.996 47	1.2365	0.795 98	462.71
10.00	1283.2	212.63	1.0417	1.2833	0.809 61	415.95
20.00	1229.7	225.76	1.0873	1.3455	0.824 07	366.79
30.00	1167.5	239.64	1.1338	1.4385	0.839 97	313.57
40.00	140.85	347.40	1.4789	1.2839	0.828 81	108.78
50.00	125.54	359.42	1.5167	1.1419	0.827 13	118.58
60.00	115.09	370.48	1.5504	1.0776	0.830 02	126.12
70.00	107.17	381.07	1.5817	1.0431	0.835 59	132.39
80.00	100.81	391.39	1.6114	1.0239	0.842 97	137.82
90.00	95.505	401.57	1.6398	1.0137	0.851 63	142.66
100.00	90.973	411.68	1.6673	1.0091	0.861 27	147.05
110.00	87.024	421.77	1.6939	1.0086	0.871 64	151.09
120.00	83.530	431.86	1.7200	1.0108	0.882 59	154.85
130.00	80.404	441.99	1.7454	1.0152	0.894 00	158.36
140.00	77.579	452.17	1.7703	1.0212	0.905 78	161.69
150.00	75.005	462.42	1.7948	1.0284	0.917 86	164.84
160.00	72.645	472.75	1.8190	1.0366	0.930 17	167.85
170.00	70.467	483.16	1.8427	1.0456	0.942 68	170.73
180.00	68.448	493.66	1.8662	1.0552	0.955 34	173.50
190.00	66.568	504.26	1.8893	1.0653	0.968 13	176.17
200.00	64.811	514.97	1.9122	1.0759	0.981 02	178.75
			$P=3000$ kPa			
Sat. liq. 57.486	910.09	285.02	1.2737	2.5894	0.898 51	152.57
Sat. vap. 57.486	260.57	345.15	1.4556	2.5003	0.891 27	93.34
−90.00	1662.3	99.85	0.551 01	1.0503	0.676 09	898.00
−80.00	1629.4	110.36	0.606 89	1.0535	0.689 47	841.28
−70.00	1596.4	120.94	0.660 28	1.0629	0.703 38	789.18
−60.00	1563.1	131.63	0.711 67	1.0767	0.717 21	740.35
−50.00	1529.1	142.48	0.761 41	1.0938	0.730 73	693.83
−40.00	1494.2	153.52	0.809 78	1.1136	0.743 91	648.85
−30.00	1458.1	164.76	0.857 02	1.1363	0.756 82	604.82
−20.00	1420.3	176.25	0.903 32	1.1621	0.769 58	561.26
−10.00	1380.5	188.02	0.948 89	1.1916	0.782 34	517.69
0.00	1338.0	200.10	0.993 96	1.2263	0.795 28	473.68
10.00	1292.0	212.57	1.0388	1.2681	0.808 60	428.67
20.00	1241.3	225.50	1.0837	1.3214	0.822 58	382.01
30.00	1183.6	239.06	1.1291	1.3947	0.837 63	332.66
40.00	1114.8	253.53	1.1761	1.5113	0.854 55	278.79
50.00	1023.5	269.70	1.2269	1.7651	0.875 30	215.96
60.00	240.25	350.64	1.4721	1.9569	0.884 92	98.72
70.00	199.48	366.62	1.5194	1.3930	0.875 07	112.72
80.00	177.78	379.64	1.5568	1.2343	0.874 25	122.24
90.00	162.93	391.57	1.5902	1.1598	0.877 46	129.78
100.00	151.69	402.94	1.6211	1.1187	0.883 11	136.13
110.00	142.68	414.00	1.6503	1.0948	0.890 42	141.67
120.00	135.20	424.87	1.6783	1.0810	0.898 94	146.62

TABLE 13. Properties of HFC-125 in the single-phase region—Continued

t °C	ρ kg/m^3	h kJ/kg	s kJ/(kg K)	C_p kJ/(kg K)	C_v kJ/(kg K)	w m/s
			$P=3000$ kPa			
130.00	128.81	435.64	1.7054	1.0737	0.908 37	151.11
140.00	123.26	446.36	1.7316	1.0708	0.918 50	155.26
150.00	118.35	457.07	1.7572	1.0711	0.929 19	159.10
160.00	113.97	467.79	1.7823	1.0738	0.940 32	162.71
170.00	110.02	478.55	1.8068	1.0784	0.951 81	166.11
180.00	106.42	489.36	1.8310	1.0843	0.963 60	169.34
190.00	103.12	500.24	1.8547	1.0914	0.975 62	172.42
200.00	100.08	511.19	1.8781	1.0993	0.987 83	175.36
			$P=4000$ kPa			
−90.00	1664.2	100.23	0.549 82	1.0496	0.676 52	903.06
−80.00	1631.5	110.73	0.605 66	1.0525	0.689 78	846.62
−70.00	1598.8	121.30	0.658 99	1.0616	0.703 58	794.84
−60.00	1565.8	131.98	0.710 31	1.0749	0.717 32	746.40
−50.00	1532.2	142.81	0.759 95	1.0915	0.730 75	700.31
−40.00	1497.7	153.82	0.808 21	1.1107	0.743 84	655.84
−30.00	1462.1	165.03	0.855 30	1.1324	0.756 65	612.44
−20.00	1425.0	176.48	0.901 42	1.1570	0.769 29	569.63
−10.00	1386.0	188.18	0.946 77	1.1849	0.781 91	526.99
0.00	1344.7	200.19	0.991 55	1.2171	0.794 66	484.15
10.00	1300.3	212.54	1.0360	1.2550	0.807 71	440.68
20.00	1251.8	225.32	1.0803	1.3016	0.821 30	396.09
30.00	1197.8	238.62	1.1249	1.3619	0.835 72	349.75
40.00	1135.4	252.64	1.1704	1.4476	0.851 47	300.66
50.00	1059.2	267.76	1.2179	1.5914	0.869 49	247.07
60.00	953.14	285.09	1.2707	1.9420	0.892 33	184.76
70.00	654.50	316.71	1.3639	9.6031	0.937 74	96.13
80.00	311.57	361.44	1.4930	2.0096	0.915 30	104.72
90.00	259.64	378.36	1.5403	1.4915	0.907 77	116.53
100.00	230.85	392.28	1.5781	1.3164	0.907 35	125.49
110.00	211.12	404.97	1.6117	1.2304	0.910 57	132.84
120.00	196.25	417.01	1.6427	1.1816	0.916 08	139.15
130.00	184.38	428.67	1.6720	1.1522	0.923 19	144.71
140.00	174.55	440.09	1.7000	1.1343	0.931 47	149.71
150.00	166.20	451.38	1.7270	1.1238	0.940 64	154.27
160.00	158.96	462.58	1.7532	1.1184	0.950 51	158.47
170.00	152.59	473.76	1.7787	1.1167	0.960 93	162.39
180.00	146.90	484.93	1.8036	1.1176	0.971 80	166.06
190.00	141.79	496.12	1.8280	1.1207	0.983 03	169.52
200.00	137.14	507.35	1.8520	1.1253	0.994 56	172.80
			$P=5000$ kPa			
−90.00	1666.1	100.61	0.548 64	1.0490	0.676 95	908.05
−80.00	1633.6	111.11	0.604 44	1.0515	0.690 09	851.89
−70.00	1601.2	121.67	0.657 72	1.0603	0.703 80	800.43
−60.00	1568.5	132.33	0.708 96	1.0732	0.717 44	752.34
−50.00	1535.2	143.14	0.758 52	1.0892	0.730 79	706.67
−40.00	1501.2	154.12	0.806 66	1.1078	0.743 79	662.69
−30.00	1466.1	165.31	0.853 62	1.1288	0.756 51	619.87
−20.00	1429.6	176.71	0.899 58	1.1524	0.769 04	577.75
−10.00	1391.4	188.36	0.944 72	1.1788	0.781 53	535.97
0.00	1351.1	200.30	0.989 23	1.2088	0.794 11	494.18
10.00	1308.0	212.55	1.0333	1.2436	0.806 93	452.06
20.00	1261.5	225.19	1.0772	1.2849	0.820 19	409.24
30.00	1210.4	238.29	1.1211	1.3361	0.834 12	365.31
40.00	1152.8	251.97	1.1655	1.4034	0.849 04	319.74

TABLE 13. Properties of HFC-125 in the single-phase region—Continued

t °C	ρ kg/m^3	h kJ/kg	s kJ/(kg K)	C_p kJ/(kg K)	C_v kJ/(kg K)	w m/s
			$P=5000$ kPa			
50.00	1085.6	266.45	1.2110	1.5008	0.865 49	271.77
60.00	1002.1	282.20	1.2590	1.6677	0.884 47	220.24
70.00	884.06	300.52	1.3131	2.0693	0.908 32	163.40
80.00	656.86	327.43	1.3903	3.5750	0.940 15	108.95
90.00	425.28	359.04	1.4787	2.3903	0.939 86	107.16
100.00	341.71	378.81	1.5324	1.6985	0.932 69	117.08
110.00	297.99	394.37	1.5736	1.4476	0.931 17	125.78
120.00	269.35	408.17	1.6092	1.3254	0.933 34	133.21
130.00	248.42	421.05	1.6415	1.2563	0.937 95	139.69
140.00	232.09	433.39	1.6717	1.2140	0.944 29	145.43
150.00	218.80	445.38	1.7004	1.1873	0.951 89	150.61
160.00	207.65	457.16	1.7279	1.1706	0.960 48	155.34
170.00	198.10	468.82	1.7545	1.1604	0.969 83	159.71
180.00	189.76	480.39	1.7804	1.1550	0.979 79	163.76
190.00	182.38	491.93	1.8055	1.1530	0.990 24	167.56
200.00	175.78	503.46	1.8302	1.1536	1.0011	171.14
			$P=6000$ kPa			
−90.00	1667.9	101.00	0.547 47	1.0484	0.677 39	912.99
−80.00	1635.7	111.49	0.603 23	1.0506	0.690 41	857.09
−70.00	1603.5	122.03	0.656 45	1.0590	0.704 02	805.93
−60.00	1571.1	132.68	0.707 63	1.0716	0.717 58	758.18
−50.00	1538.2	143.48	0.757 10	1.0871	0.730 84	712.91
−40.00	1504.5	154.44	0.805 14	1.1052	0.743 76	669.40
−30.00	1469.9	165.59	0.851 97	1.1254	0.756 39	627.12
−20.00	1434.0	176.95	0.897 77	1.1480	0.768 82	585.66
−10.00	1396.5	188.55	0.942 72	1.1731	0.781 19	544.66
0.00	1357.2	200.42	0.986 99	1.2014	0.793 62	503.83
10.00	1315.4	212.59	1.0307	1.2335	0.806 24	462.89
20.00	1270.6	225.11	1.0742	1.2707	0.819 23	421.59
30.00	1221.9	238.03	1.1175	1.3152	0.832 76	379.66
40.00	1168.0	251.45	1.1611	1.3704	0.847 06	336.81
50.00	1107.0	265.50	1.2052	1.4431	0.862 47	292.75
60.00	1035.4	280.41	1.2507	1.5474	0.879 48	247.21
70.00	946.63	296.66	1.2987	1.7189	0.898 87	200.22
80.00	826.50	315.33	1.3523	2.0553	0.921 59	153.77
90.00	655.63	338.48	1.4169	2.5360	0.944 06	120.33
100.00	497.57	362.76	1.4829	2.1922	0.950 38	115.90
110.00	408.93	382.25	1.5345	1.7480	0.948 85	122.35
120.00	356.82	398.44	1.5762	1.5141	0.948 99	129.70
130.00	321.82	412.88	1.6125	1.3858	0.951 62	136.53
140.00	296.13	426.32	1.6454	1.3092	0.956 27	142.70
150.00	276.11	439.15	1.6761	1.2609	0.962 48	148.30
160.00	259.87	451.59	1.7052	1.2294	0.969 89	153.41
170.00	246.30	463.78	1.7330	1.2088	0.978 25	158.11
180.00	234.70	475.79	1.7598	1.1956	0.987 36	162.47
190.00	224.62	487.71	1.7858	1.1877	0.997 08	166.54
200.00	215.72	499.56	1.8111	1.1837	1.0073	170.36
			$P=7000$ kPa			
−90.00	1669.8	101.39	0.546 31	1.0478	0.677 83	917.87
−80.00	1637.8	111.87	0.602 04	1.0498	0.690 74	862.23
−70.00	1605.8	122.40	0.655 21	1.0578	0.704 25	811.35
60.00	1573.7	133.04	0.706 31	1.0700	0.717 73	763.94
−50.00	1541.1	143.81	0.755 71	1.0851	0.730 91	719.04
−40.00	1507.8	154.75	0.803 65	1.1026	0.743 75	675.97

TABLE 13. Properties of HFC-125 in the single-phase region—Continued

t °C	ρ kg/m^3	h kJ/kg	s kJ/(kg K)	C_p kJ/(kg K)	C_v kJ/(kg K)	w m/s
			$P=7000$ kPa			
−30.00	1473.6	165.87	0.850 36	1.1222	0.756 29	634.21
−20.00	1438.3	177.20	0.896 01	1.1439	0.768 63	593.35
−10.00	1401.5	188.76	0.940 79	1.1679	0.780 89	553.08
0.00	1363.0	200.57	0.984 83	1.1946	0.793 18	513.12
10.00	1322.3	212.66	1.0283	1.2244	0.805 63	473.25
20.00	1279.0	225.07	1.0714	1.2584	0.818 39	433.28
30.00	1232.4	237.85	1.1142	1.2977	0.831 59	393.02
40.00	1181.5	251.05	1.1571	1.3445	0.845 41	352.36
50.00	1125.1	264.77	1.2002	1.4021	0.860 07	311.21
60.00	1061.1	279.15	1.2440	1.4764	0.875 85	269.65
70.00	986.62	294.39	1.2891	1.5783	0.893 08	228.08
80.00	896.64	310.87	1.3364	1.7278	0.912 02	187.81
90.00	784.86	329.18	1.3875	1.9434	0.932 08	152.67
100.00	654.16	349.60	1.4430	2.1039	0.949 03	130.85
110.00	537.66	370.11	1.4972	1.9514	0.957 13	126.15
120.00	457.60	388.34	1.5442	1.7021	0.959 96	129.92
130.00	404.17	404.41	1.5846	1.5254	0.962 56	135.74
140.00	366.27	419.06	1.6205	1.4130	0.966 46	141.71
150.00	337.73	432.80	1.6534	1.3406	0.971 77	147.37
160.00	315.21	445.95	1.6841	1.2926	0.978 31	152.65
170.00	296.81	458.71	1.7132	1.2603	0.985 88	157.54
180.00	281.38	471.20	1.7411	1.2385	0.994 29	162.10
190.00	268.16	483.50	1.7679	1.2241	1.0034	166.36
200.00	256.66	495.69	1.7940	1.2150	1.0131	170.35
			$P=8000$ kPa			
−90.00	1671.6	101.78	0.545 17	1.0473	0.678 28	922.69
−80.00	1639.8	112.25	0.600 85	1.0489	0.691 08	867.30
−70.00	1608.1	122.78	0.653 97	1.0567	0.704 50	816.70
−60.00	1576.2	133.40	0.705 02	1.0685	0.717 89	769.60
−50.00	1543.9	144.15	0.754 33	1.0832	0.730 99	725.07
−40.00	1511.0	155.07	0.802 18	1.1002	0.743 75	682.42
−30.00	1477.3	166.17	0.848 77	1.1192	0.756 22	641.14
−20.00	1442.4	177.46	0.894 29	1.1401	0.768 47	600.86
−10.00	1406.3	188.97	0.938 90	1.1631	0.780 63	561.25
0.00	1368.6	200.73	0.982 74	1.1883	0.792 80	522.09
10.00	1329.0	212.75	1.0260	1.2163	0.805 09	483.18
20.00	1287.0	225.07	1.0687	1.2475	0.817 64	444.38
30.00	1242.1	237.71	1.1111	1.2829	0.830 57	405.57
40.00	1193.7	250.74	1.1534	1.3235	0.844 00	366.71
50.00	1140.9	264.21	1.1957	1.3712	0.858 10	327.85
60.00	1082.4	278.20	1.2383	1.4283	0.873 03	289.17
70.00	1016.6	292.82	1.2816	1.4987	0.888 95	251.16
80.00	941.52	308.23	1.3259	1.5874	0.905 94	214.80
90.00	854.78	324.64	1.3717	1.6987	0.923 71	182.00
100.00	756.07	342.24	1.4195	1.8181	0.940 97	156.02
110.00	652.73	360.78	1.4685	1.8688	0.954 91	140.71
120.00	561.44	379.12	1.5158	1.7804	0.963 65	136.37
130.00	491.87	396.20	1.5587	1.6337	0.969 07	138.44
140.00	440.92	411.88	1.5971	1.5088	0.973 82	142.90
150.00	402.72	426.49	1.6320	1.4188	0.979 12	147.98
160.00	373.02	440.35	1.6644	1.3561	0.985 32	153.06
170.00	349.13	453.68	1.6948	1.3124	0.992 43	157.93
180.00	329.37	466.64	1.7238	1.2820	1.0004	162.55
190.00	312.67	479.35	1.7515	1.2609	1.0090	166.90
200.00	298.28	491.88	1.7783	1.2466	1.0182	171.00

TABLE 13. Properties of HFC-125 in the single-phase region—Continued

t °C	ρ kg/m^3	h kJ/kg	s kJ/(kg K)	C_p kJ/(kg K)	C_v kJ/(kg K)	w m/s
			$P=9000$ kPa			
−90.00	1673.4	102.17	0.544 03	1.0468	0.678 74	927.46
−80.00	1641.8	112.63	0.599 68	1.0481	0.691 42	872.31
−70.00	1610.3	123.15	0.652 75	1.0556	0.704 75	821.98
−60.00	1578.7	133.76	0.703 73	1.0671	0.718 05	775.18
−50.00	1546.7	144.50	0.752 97	1.0814	0.731 08	731.00
−40.00	1514.2	155.39	0.800 73	1.0979	0.743 77	688.75
−30.00	1480.8	166.46	0.847 22	1.1163	0.756 16	647.93
−20.00	1446.5	177.73	0.892 61	1.1365	0.768 34	608.17
−10.00	1411.0	189.20	0.937 06	1.1585	0.780 40	569.19
0.00	1374.0	200.90	0.980 70	1.1826	0.792 45	530.77
10.00	1335.3	212.86	1.0237	1.2089	0.804 61	492.73
20.00	1294.5	225.09	1.0661	1.2379	0.816 98	454.97
30.00	1251.2	237.63	1.1082	1.2700	0.829 67	417.42
40.00	1204.9	250.50	1.1500	1.3060	0.842 79	380.08
50.00	1155.0	263.76	1.1916	1.3467	0.856 45	343.06
60.00	1100.6	277.46	1.2334	1.3930	0.870 75	306.60
70.00	1041.0	291.64	1.2753	1.4461	0.885 79	271.17
80.00	974.95	306.40	1.3177	1.5071	0.901 57	237.53
90.00	901.76	321.81	1.3608	1.5764	0.917 90	206.88
100.00	821.33	337.95	1.4046	1.6504	0.934 19	180.85
110.00	735.80	354.78	1.4491	1.7119	0.949 24	161.41
120.00	651.40	372.02	1.4935	1.7226	0.961 56	150.04
130.00	576.73	389.00	1.5361	1.6635	0.970 67	146.20
140.00	516.39	405.17	1.5758	1.5706	0.977 67	147.24
150.00	469.28	420.43	1.6123	1.4829	0.984 01	150.61
160.00	432.27	434.89	1.6461	1.4135	0.990 55	154.87
170.00	402.59	448.76	1.6777	1.3618	0.997 65	159.36
180.00	378.21	462.18	1.7077	1.3242	1.0054	163.81
190.00	357.76	475.28	1.7363	1.2971	1.0138	168.12
200.00	340.30	488.15	1.7637	1.2779	1.0227	172.24
			$P=10\,000$ kPa			
−90.00	1675.2	102.56	0.542 90	1.0463	0.679 20	932.18
−80.00	1643.8	113.02	0.598 51	1.0474	0.691 77	877.26
−70.00	1612.5	123.52	0.651 54	1.0545	0.705 01	827.19
−60.00	1581.2	134.12	0.702 47	1.0657	0.718 23	780.68
−50.00	1549.5	144.85	0.751 64	1.0796	0.731 19	736.83
−40.00	1517.2	155.72	0.799 31	1.0957	0.743 81	694.96
−30.00	1484.3	166.77	0.845 69	1.1136	0.756 13	654.57
−20.00	1450.4	178.00	0.890 96	1.1331	0.768 22	615.32
−10.00	1415.5	189.43	0.935 26	1.1543	0.780 20	576.92
0.00	1379.2	201.09	0.978 73	1.1773	0.792 15	539.17
10.00	1341.3	212.99	1.0215	1.2022	0.804 19	501.93
20.00	1301.6	225.14	1.0637	1.2292	0.816 40	465.10
30.00	1259.7	237.58	1.1054	1.2588	0.828 89	428.66
40.00	1215.2	250.33	1.1468	1.2911	0.841 74	392.63
50.00	1167.7	263.41	1.1879	1.3267	0.855 04	357.14
60.00	1116.7	276.87	1.2289	1.3656	0.868 87	322.46
70.00	1061.5	290.74	1.2699	1.4081	0.883 27	289.01
80.00	1001.8	305.04	1.3110	1.4540	0.898 22	257.40
90.00	937.23	319.83	1.3523	1.5027	0.913 59	228.47
100.00	867.95	335.10	1.3938	1.5526	0.929 02	203.20
110.00	795.02	350.87	1.4355	1.5987	0.943 91	182.63
120.00	720.99	367.02	1.4771	1.6285	0.957 43	167.71

TABLE 13. Properties of HFC-125 in the single-phase region—Continued

t °C	ρ kg/m^3	h kJ/kg	s kJ/(kg K)	C_p kJ/(kg K)	C_v kJ/(kg K)	w m/s
			$P=10\,000$ kPa			
130.00	650.19	383.32	1.5180	1.6242	0.968 90	158.92
140.00	587.23	399.38	1.5574	1.5816	0.978 29	155.57
150.00	534.44	414.89	1.5945	1.5189	0.986 32	156.01
160.00	491.36	429.76	1.6292	1.4565	0.993 82	158.55
170.00	456.25	444.05	1.6618	1.4037	1.0014	162.09
180.00	427.30	457.87	1.6927	1.3623	1.0093	166.03
190.00	403.05	471.33	1.7220	1.3309	1.0177	170.07
200.00	382.41	484.51	1.7502	1.3077	1.0265	174.05
			$P=15\,000$ kPa			
−90.00	1683.8	104.52	0.537 38	1.0441	0.681 60	955.00
−80.00	1653.3	114.96	0.592 85	1.0440	0.693 63	901.15
−70.00	1623.1	125.42	0.645 67	1.0498	0.706 42	852.24
−60.00	1592.9	135.97	0.696 34	1.0596	0.719 27	807.05
−50.00	1562.5	146.62	0.745 19	1.0719	0.731 89	764.66
−40.00	1531.8	157.41	0.792 48	1.0861	0.744 19	724.44
−30.00	1500.6	168.35	0.838 42	1.1018	0.756 19	685.94
−20.00	1468.8	179.45	0.883 16	1.1187	0.767 96	648.81
−10.00	1436.2	190.73	0.926 85	1.1367	0.779 58	612.82
0.00	1402.8	202.19	0.969 59	1.1557	0.791 12	577.82
10.00	1368.4	213.84	1.0115	1.1756	0.802 68	543.70
20.00	1332.9	225.70	1.0527	1.1964	0.814 32	510.43
30.00	1296.1	237.77	1.0931	1.2180	0.826 11	478.01
40.00	1258.0	250.07	1.1330	1.2402	0.838 10	446.51
50.00	1218.4	262.58	1.1724	1.2628	0.850 32	416.07
60.00	1177.3	275.32	1.2112	1.2853	0.862 80	386.86
70.00	1134.7	288.29	1.2495	1.3074	0.875 54	359.12
80.00	1090.7	301.47	1.2874	1.3284	0.888 52	333.11
90.00	1045.4	314.85	1.3248	1.3479	0.901 70	309.12
100.00	999.15	328.42	1.3616	1.3655	0.915 00	287.36
110.00	952.22	342.15	1.3979	1.3810	0.928 31	267.99
120.00	905.08	356.03	1.4337	1.3946	0.941 52	251.06
130.00	858.17	370.04	1.4689	1.4064	0.954 49	236.56
140.00	812.00	384.15	1.5035	1.4160	0.967 13	224.43
150.00	767.09	398.35	1.5374	1.4226	0.979 33	214.62
160.00	724.02	412.59	1.5707	1.4251	0.991 07	207.09
170.00	683.34	426.83	1.6032	1.4226	1.0023	201.74
180.00	645.55	441.03	1.6349	1.4152	1.0132	198.38
190.00	610.96	455.13	1.6656	1.4039	1.0237	196.74
200.00	579.65	469.10	1.6955	1.3905	1.0341	196.49
			$P=20\,000$ kPa			
−90.00	1692.0	106.51	0.532 06	1.0425	0.684 11	976.68
−80.00	1662.4	116.92	0.587 42	1.0412	0.695 63	923.75
−70.00	1633.0	127.35	0.640 07	1.0459	0.708 00	875.84
−60.00	1603.8	137.85	0.690 52	1.0545	0.720 50	831.74
−50.00	1574.6	148.45	0.739 11	1.0655	0.732 82	790.57
−40.00	1545.1	159.17	0.786 10	1.0783	0.744 84	751.70
−30.00	1515.4	170.02	0.831 67	1.0924	0.756 58	714.68
−20.00	1485.2	181.02	0.876 00	1.1075	0.768 09	679.20
−10.00	1454.5	192.18	0.919 21	1.1233	0.779 43	645.04
0.00	1423.3	203.49	0.961 41	1.1398	0.790 69	612.04
10.00	1391.4	214.97	1.0027	1.1568	0.801 93	580.13
20.00	1358.8	226.63	1.0431	1.1742	0.813 20	549.25
30.00	1325.4	238.46	1.0828	1.1918	0.824 58	519.42
40.00	1291.2	250.46	1.1218	1.2095	0.836 08	490.68

TABLE 13. Properties of HFC-125 in the single-phase region—Continued

t °C	ρ kg/m^3	h kJ/kg	s kJ/(kg K)	C_p kJ/(kg K)	C_v kJ/(kg K)	w m/s
			$P = 20\,000$ kPa			
50.00	1256.3	262.65	1.1601	1.2270	0.847 75	463.12
60.00	1220.5	275.00	1.1977	1.2440	0.859 59	436.85
70.00	1184.1	287.53	1.2348	1.2602	0.871 61	412.01
80.00	1147.0	300.20	1.2712	1.2753	0.883 82	388.73
90.00	1109.5	313.03	1.3070	1.2891	0.896 17	367.14
100.00	1071.7	325.98	1.3422	1.3013	0.908 65	347.35
110.00	1033.8	339.05	1.3767	1.3121	0.921 20	329.39
120.00	996.11	352.22	1.4107	1.3214	0.933 79	313.27
130.00	958.78	365.47	1.4440	1.3296	0.946 37	298.92
140.00	922.04	378.81	1.4766	1.3370	0.958 88	286.24
150.00	886.07	392.21	1.5087	1.3437	0.971 30	275.13
160.00	851.03	405.68	1.5401	1.3498	0.983 59	265.47
170.00	817.06	419.20	1.5710	1.3553	0.995 74	257.18
180.00	784.29	432.78	1.6013	1.3601	1.0077	250.17
190.00	752.86	446.40	1.6310	1.3638	1.0196	244.39
200.00	722.89	460.06	1.6602	1.3664	1.0312	239.78

10. References

Baroncini, C., G. Giuliani, and F. Polonara, "Thermodynamic Properties of Refrigerant R125 (CHF_2CF_3): An Experimental Study," 3rd World Conference on Experimental Heat Transfer, Fluid Mechanics and Thermodynamics Vol. 2, 1774 (1993).

Bignell, C. M. and P. J. Dunlop, J. Chem. Phys. **98**, 4889 (1993).

Boyes, S. J. and L. A. Weber, J. Chem. Thermodyn. **27**, 163 (1995).

Chen, S. S., A. S. Rodgers, J. Chao, R. C. Wilhoit, and B. J. Zwolinski, J. Phys. Chem. Ref. Data **4**, 441 (1975).

de Vries, B., *Thermodynamische Eigenschasften der Alternativen Kaltemittel R-32, R-125 und R-143a—Messungen und Zustandsgleichungen-, Forsch.-Ber.* DKV No. 55 (DKV, Stuttgart, Germany, 1997).

Defibaugh, D. R. and G. Morrison, Fluid Phase Equilibria **80**, 157 (1992).

Duarte-Garza, H. A. and J. W. Magee, Int. J. Thermophys. **18**, 173 (1997a).

Duarte-Garza, H. A., C. E. Stouffer, K. R. Hall, J. C. Holste, K. N. Marsh, and B. E. Gammon, J. Chem. Eng. Data **42**, 745 (1997b).

Fukushima, M. and S. Ohotoshi, Thermodynamic Properties of HFC-125, 13th Japan Symposium Thermophys. Prop. 49 (1992).

Gillis, K. A., Int. J. Thermophys. **18**, 73 (1997).

Gorenflo, D., R. Koester, and G. Herres, 1996 (private communication).

Grebenkov, A. J., Yu. G. Kotelevsky, V. V. Saplitza, O. V. Beljaeva, T. A. Zajatz, and B. D. Timofeev, Experimental Study of Thermal Conductivity of Some Ozone Safe Refrigerants and Speed of Sound in their Liquid Phase. Proc. CFC's: The Day After, IIR Comm. B1, B2, E1, E2 21, 1994.

Higashi, Y., Int. J. Refrig. **17**, 524 (1994).

Hozumi, T., H. Sato, and K. Watanabe, Int. J. Thermophys. **17**, 587 (1996).

Kan, T., G. Yasuda, M. Suzuki, H. Sato, and K. Watanabe, Isobaric Heat Capacity of Liquid R-125. Proc. of the 33rd National Heat Transfer Symposium of Japan, Nigata, Japan 169, 1996.

Kilner, J. and R. J. B. Craven, Comparisons of Equations of State with Experimental Data for R32 and R125, IUPAC Thermodynamic Tables Project Center, Imperial College, London, Final Report to the International Energy Agency—Annex 18, 1996.

Kraft, K. and A. Leipertz, Int. J. Thermophys. **15**, 387 (1994).

Kuwabara, S., H. Aoyama, H. Sato, and K. Watanabe, J. Chem. Eng. Data **40**, 112 (1995).

Lueddecke, T. O. and J. W. Magee, Int. J. Thermophys. **17**, 823 (1996).

Magee, J. W., Int. J. Thermophys. **17**, 803 (1996).

Monluc, Y., T. Sagawa, H. Sato, and K. Watanabe, Thermodynamic Properties of HFC-125, Proc. 12th Japan Symp. Thermophys. Prop. 65, 1991.

Nagel, M. and K. Bier, Vapor–Liquid Equilibrium of New Refrigerant Mixtures as Alternatives to R22 and R502, DKV-Tagungsbericht 20, Band II.1 39, 1993.

Oguchi, K., A. Murano, K. Omata, and N. Yada, Int. J. Thermophys. **17**, 55 (1996).

Piao, C.-C. and M. Noguchi, "Thermodynamic Properties of HFC-32 (Difluoromethane)," Int. J. Refrig., 1996a (submitted).

Piao, C.-C. and M. Noguchi, Fluid Phase Equilibria **125**, 45 (1996b).

Piao, C.-C., M. Noguchi, H. Sato, and K. Watanabe, Final Report to the IEA-Annex 18, 1993.

Piao, C.-C., M. Noguchi, H. Sato, and K. Watanabe, ASHRAE Trans. **100**, 358 (1994).

Sagawa, T., Thermodynamic Properties of HFC-125 by a Constant-Volume Method. M.S. Thesis, Keio University (1994a).

Sagawa, T., H. Sato, and K. Watanabe, High Temp.-High Press. **26**, 193 (1994b).

Schmidt, J. W. and M. R. Moldover, J. Chem. Eng. Data **39**, 39 (1994).

Singh, R. R., F. A. E. Lund, and J. R. Shankland, Thermophysical Properties of HFC-32, HFC-125 and HFC-32/HFC-125, Proc. of the CFC and Halon International Conference 451, 1991.

Takagi, T., J. Chem. Eng. Data **41**, 1325 (1996).

Tillner-Roth, R. and A. Yokozeki, J. Phys. Chem. Ref. Data **26**, 1273 (1997).

Tillner-Roth, R. and H. D. Baehr, J. Phys. Chem. Ref. Data **23**, 657 (1994).

Tsvetkov, O. B., A. V. Kletski, Yu. A. Laptev, A. J. Asambaev, and I. A. Zausaev, Int. J. Thermophys. **16**, 1185 (1995).

Weber, L. A. and A. M. Silva, J. Chem. Eng. Data **39**, 808 (1994).

Widiatmo, J. V., H. Sato, and K. Watanabe, J. Chem. Eng. Data **39**, 304 (1994).

Wilson, L. C., W. V. Wilding, G. M. Wilson, R. L. Rowley, V. M. Felix, and T. Chisolm-Carter, Fluid Phase Equilibria **80**, 167 (1992).

Ye, F., H. Sato, and K. Watanabe, J. Chem. Eng. Data **40**, 148 (1995).

Younglove, B. A. and M. O. McLinden, J. Phys. Chem. Ref. Data **23**, 731 (1994).

Zhang, H.-L., H. Sato, and K. Watanabe, Second Virial Coefficients for R-32, R-125, R-134a, R143a, R-152a, and their Binary Mixtures. Proc. 19th Int. Congress Refrig., The Hague, The Netherlands **IVA**, 622, 1995.

Zhang, H.-L., H. Sato, and K. Watanabe, J. Chem. Eng. Data **41**, 1401 (1996).